MEASUREMENT OF THE WAVE HEIGHT PRODUCED BY THE FORCED HEAVING OF THE CYLINDERS

TASAI, Fukuzo
Research Institute for Applied Mechanics, Kyushu University

https://doi.org/10.5109/7164776

出版情報：Reports of Research Institute for Applied Mechanics. 8 (29), pp.279-310, 1960. 九州大学応用力学研究所
バージョン：
権利関係：

Reports of Research Institute for Applied Mechanics
Vol. VIII, No. 29, 1960

MEASUREMENT OF THE WAVE HEIGHT PRODUCED BY THE FORCED HEAVING OF THE CYLINDERS

By Fukuzō TASAI

ABSTRACT. We measured the two dimensional progressive wave height produced by forced heaving of the miscelanous cylinders, and then compared the amplitude ratio $\bar{A}$ with the F. Ursell's results [1] and author's theoretical calculations [2]. In general, the measured $\bar{A}$ was in good coincidence with that of the theoretical results. Then the author studied the Wedge effect, the effect of the variation of the section contour from the Lewis form and the effect of heaving amplitude. These are shown in many figures in this paper.

1. Preface

It is essential to know the sectional damping force for the calculation of the damping force of heaving and pitching of a ship by the Strip Method. This sectional damping force may be easily given if the progressive wave height produced by the heaving of the unlimited cylinder is estimated, provided that neglecting the frictional force the damping force is proportionate to the heaving velocity. Namely, taking the amplitude of the progressive wave height by η, heaving amplitude by S, the ratio between them is indicated by $\bar{A} = \eta/S$ and using the ratio the sectional damping force is calculated by the equation,

$$N = \frac{\rho g^2}{\omega^3} \cdot \bar{A}^2$$

where ρ = fluid density,
g = acceleration of gravity,
ω = wave circular frequency,
N = damping force/heaving velocity.

Theoretically accurate calculation of $\bar{A}$ for the circular cylinder was given by F. Ursell [1] and for the Lewis form by the author [2] respectively. In order to calculate they linearised the free surface condition by neglecting the viscosity and surface tension and by assuming the forced heaving amplitude being small as always done at the wave theory. Therefore the difference between the theoretical value and actual $\bar{A}$ having various finite heaving amplitude is determined by the experiment. Lewis Form calculated by the author in [2] was wall-sided on the water line. However there are many cases of the non-wall sided in ship-shaped

section. Generally it is very difficult to treat them theoretically. Damping force N of a certain section could be calculated approximately from [2], supposing that the value of N is equal to that of Lewis Form whose area, draught and the width of water line are respectively equal to the value of that section. But in this case the influence of variation from Lewis form over the value of $\bar{A}$ is not yet eliminated.

To detect these influence, two-dimensional progressive wave height which was produced by forced heaving of the cylinders, was measured. H. Holstein [3] is the only person that have done those measurements before. He, using the wave profile board scored with 5 mm section, measured the two-dimensional progressive wave height which was generated by the forced heaving of the rectangular cylinder with rounded corner changing the draught variously.

In this experiment he used a warter tank the length of which was very short ($L = 3.00\ m$, $B = 0.7\ m$, $D = 0.5\ m$), so that the reflective and the standing waves would have exerted great influence over the wave profile. But it is not clear how he had treated them. So his measurements are supposed not to be adequate to compare with the theoretical one. To compare it with the theoretical calculation accurately the author had done the experiment changing the amplitude of the plunger variously, first, on the circular cylinder. And to know the influence above-mentioned the test was exerted on the trianglar cylinder, rectangular cylinder with rounded corner and that having ship-shaped section.

Now I should like to present the results of these experiments.

2. Experimental Apparatus and Measuring Method

The test was held in the water tank being $L = 60$ m, $B = 1.5$ m, $D = 1.5$ m (See Photo. 1).

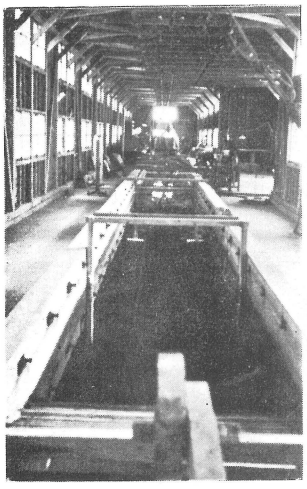

Photo 1. General view of the water tank.

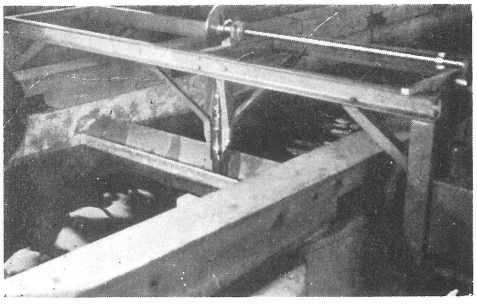

Photo 2. Forced heaving apparatus.

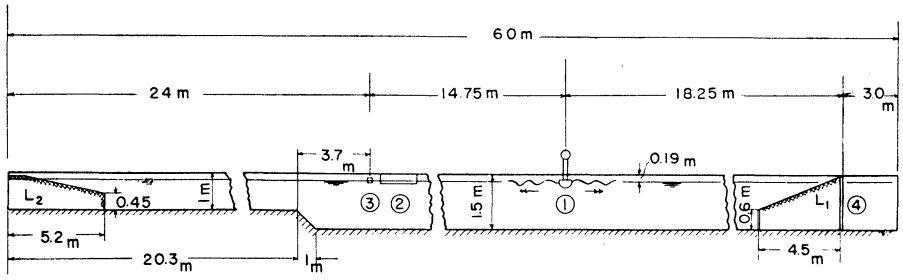

Fig 1. Water tank and general arrangement of experimental apparatus

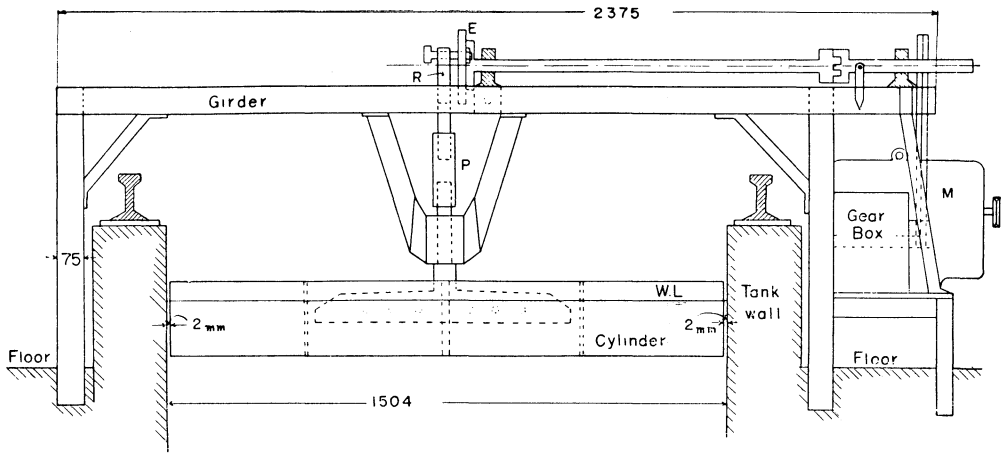

Fig. 2. Forced heaving apparatus.

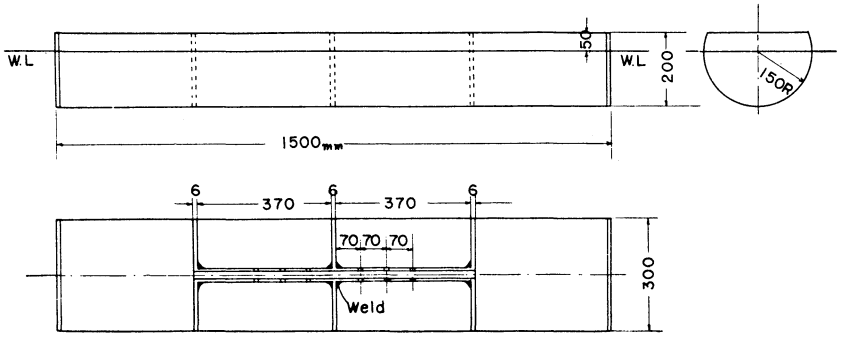

Fig. 3. Heaving cylinder (duralumin).

The explanation of the experimental apparatus and measuring method is briefly written in those that follow.

2. 1 Forced Heaving Apparatus

Fig. 1 shows the general arrangement of all the apparatus. Fig. 2 and Photo. 2 illustrate the forced heaving apparatus. Plunger P was operated by the electric motor M, eccentric apparatus E and connecting rod R. The amplitude could be verified by 70 mm. The wave making cylinder shown in Fig. 3 was made of duralumin of 150 mm in semi-diameter and 1 mm in thickness. The dimension of the other cylinders is elucidated in the figures of the experimental results. The clearance of 2 mm ~ 3 mm was found between the cylinder and the water tank wall. These formed a plunger type wave making machine.

2. 2 Wave Damper

Being elucidated in Fig. 1 and photo. 3a, 3b, there are wave-dampers at both ends of the water tank. L_2 is ready made one operated fairly well because of the whole surface of which being covered with hemp-palm brushes. The apparatus L_1 is the latticed one which is newly settled for this experiment. The apparatus is in the following: The front wall of L_1 is made of the hemp-palm brushes packed in the frame of 60 cm in height. A board is put on the wall with the inclination of 12°. And then square timbers of 30 mm is arranged like the latticed frame, having the clearance of 10 mm between the board above-mentioned.

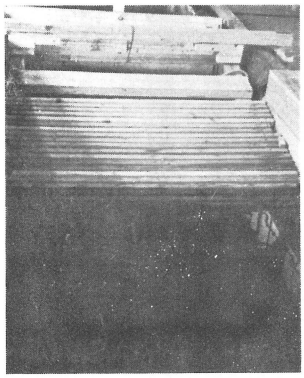

Photo. 3 (a) Wave damper. (L_1)

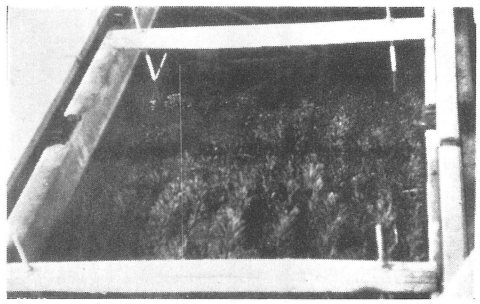

Photo. 3 (b) Wave damper. (L_2)

As the reflexion experiment, produced waves were recorded by operating the plunger a few times.

After a group of the waves passed, water surface became still. Soon after reflective waves with long period appeared gradually lessening its period. Though wave height of the reflective wave was generally very small, wave height having the period near the plunger period was higher than the other part. The time required for the appearance of the main reflective waves was almost estimated from the travelling distance of the waves and the group velocity of the wave with plunger period. Travelling distance of the wave from plunger to measuring float via the apparatus L_1 was about 42 m ~ 50 m.

Table 1 indicates the time required for the appearance of the main reflective waves on the three plunger periods.

Table 1.

Tw (sec)	1.22	1.0	0.636
t_1 (sec)	40~53	58~62	95~100
t_2 (sec)	44~51	54~64	87~100

Tw = Heaving period of the plunger
t_1, t_2 = The time required to produce the main reflective waves after operating the plunger
t_1 is the measured value, t_2 the calculated value

Main reflective wave height generated by the operation of L_1 was under 5 % of the theoretical regular one for that period. For the L_2, the travelling distance of waves being about 53 m~60 m, the reflective waves at $T_w = 1.0$ and 0.636 by L_1 and L_2 was supposed to be recorded separately, but we could merely obtain the record by L_1. Reflection by L_2 is supposed to be very small.

2. 3 Wave-Height Measuring Apparatus and Measuring Method.

Two methods were used for recording the wave height. The first one was float-type wave height recorder which was small one (15 cm × 2 cm × 2 cm) of plastics. Fig. 4 and Photo. 5a shows its appearance. As illustrated in Fig. 4,

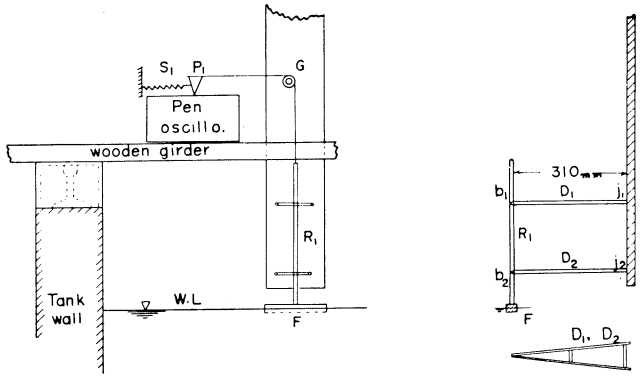

Fig. 4. Apparatus for measuring wave height.

frames D_1 and D_2 were respectively revolved round the hinges j_1 and j_2. Float F with vertical axis R_1 nearly took heaving motion. Then a fine tungsten wire $\left(\frac{2.5}{100}\text{mm}\right)$ and a pulley was used to combine the rod R_1 and the pen P_1. The wire was, moreover, pulled by the spring S_1 with statical tension of 2 gr. The measured average free heaving period of the float was 0.255 sec. The float having

such short period was designed taking into consideration the frequency of the forced having in our test, namely, wave frequency. Heaving displacement of F was recorded by P_1 through the tungsten wire and the pulley (See Photo. 5b). Pen P_1 was desinged not to move circularly but linearly. In the range of the

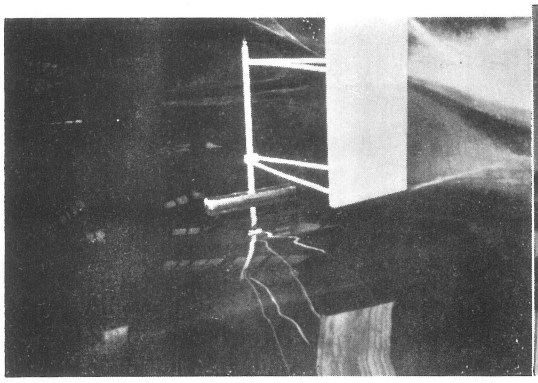

Photo. 5 (a). Float for measuring wave height.

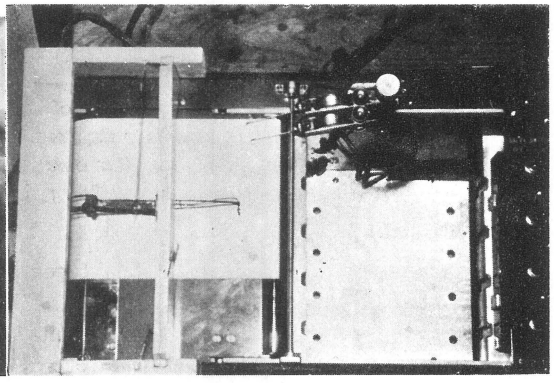

Photo. 5 (b). Pen Recorder.

heaving displacement of F in this test, the dynamical change of tension was so negligible that pen P_1 worked very good in recording the displacement of the float F. The recorded wave height was divided by mangification factor Y and reduced to the corrected value. Some of the measured ones are shown in Photo. 6 and the $\bar{A}$ (corrected) is the one divided by Y.

Photo. 6. Examples of record.

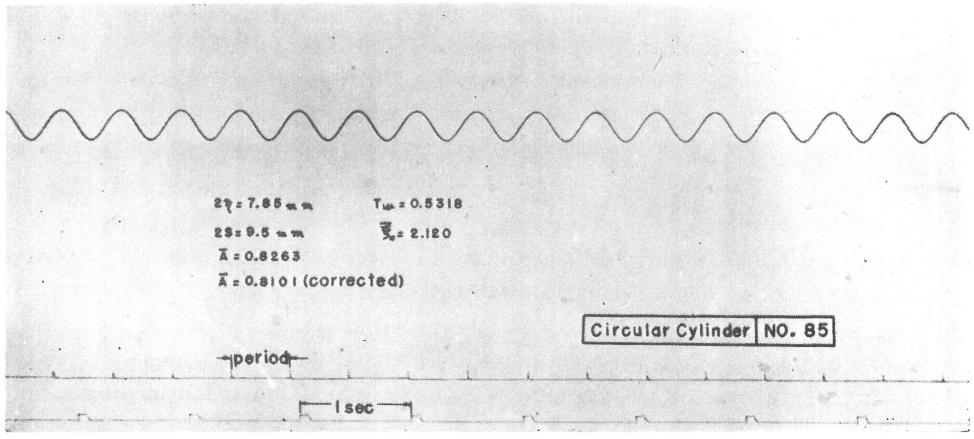

Then turn to the second method.

Illustrated in Photo. 7, wave profile scale board (200 cm×30 cm) was hunged in

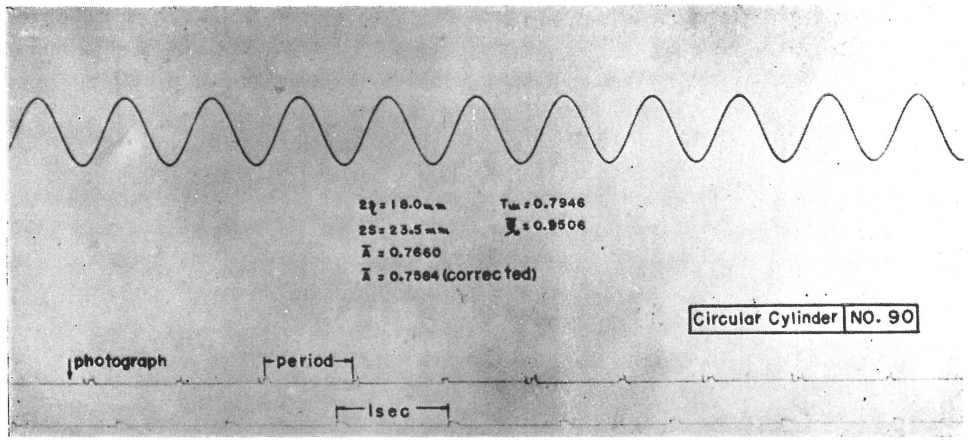
2ζ = 18.0 m m
2S = 23.5 m m
Ā = 0.7660
Ā = 0.7564 (corrected)
T_ω = 0.7946
$\bar{\xi}_o$ = 0.9506
Circular Cylinder NO. 90
photograph
period
1 sec

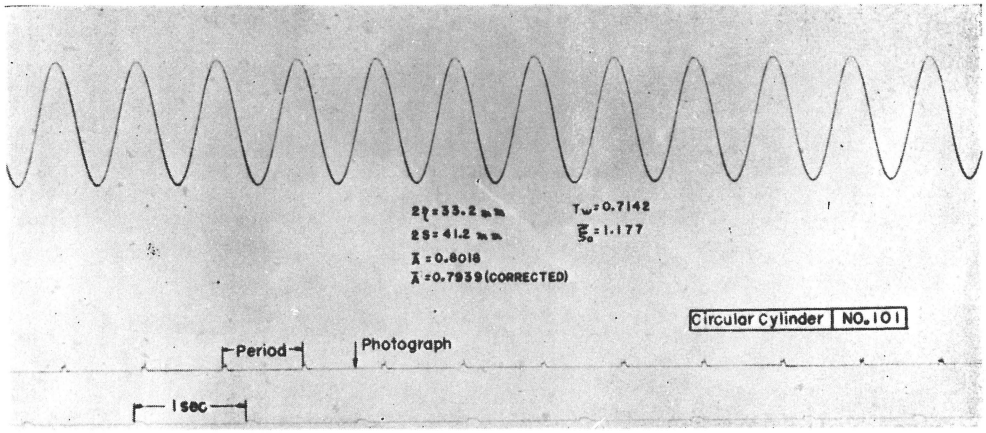
2ζ = 33.2 m m
2S = 41.2 m m
Ā = 0.8018
Ā = 0.7939 (CORRECTED)
T_ω = 0.7142
$\bar{\xi}_o$ = 1.177
Circular Cylinder NO. 101
Period
Photograph
1 sec

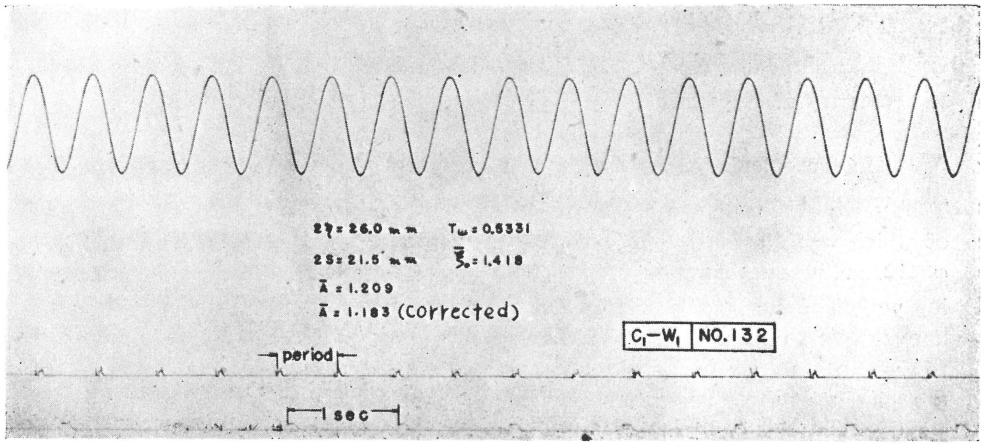
2ζ = 26.0 m m
2S = 21.5 m m
Ā = 1.209
Ā = 1.183 (corrected)
T_ω = 0.5331
$\bar{\xi}_o$ = 1.418
C_1–W_1 NO. 132
period
1 sec

the water tank apart from the tank wall by 10 cm. And photographs were taken. Then projecting the nega film on the screen we could obtain the wave height by using the vertical scale, though accurate data could not be given owing to the enlargement of photo. But the difference between the value and the measured one by the float was merely $2 \sim 3\,\%$ (See Fig. 5). The data furnished by the float was used for the measurement of the wave height, while the photographs were employed for the sake of checking the experiments and observing the waveprofile. The measuring point of the wave height being 15 m apart from the plunger, the influence of the standing wave was so small as to be negligible in practice.

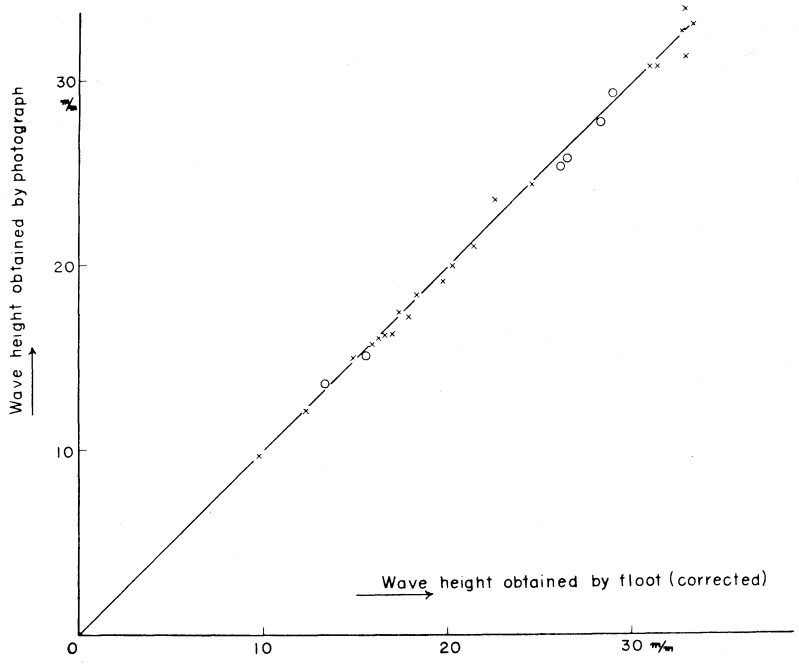

Fig. 5.

3. Summary of Experiment

In the calculation [2], $A=\eta/S$ is indicated as the function of $\xi_0=\frac{\omega^2}{g}\cdot\frac{B}{2}$. The value B denote the breadth of the section on the water line, the maximum of which was 30 cm in our experiment. The experiment was limited within $4<\omega<12$, taking consideration of the depth of the water-tank (1.3 m), natural heaving period of the float F and $\xi_0<2.5$ which is sufficient for the calculation of the damping force of a ship. The heaving amplitude was varied widely from 5 mm to 35 mm. At the first place motor was operated with constant rotation before the clutch of the plunger was put on. Then the plunger was worked with constant period and amplitude. While time and period of the plunger began to be

marked on the recording paper. Long waves were begun to be recorded gradually and the waves with the plunger period appeared soon after. And finally photographs were taken after the wave height record had been obtained with regularity. These measurement should be done before the arrival of the main reflective wave for each ω. 10 minutes was taken for the interval of each test in order to calm down the tank water. In this case the reproducibility of the experiment was very good.

4. Results of the Experiment

The length of the generated progressive waves were within 3.5 m$>\lambda>$0.4 m and as shown in photo. 6, 7, they generally approximated to the sine wave.

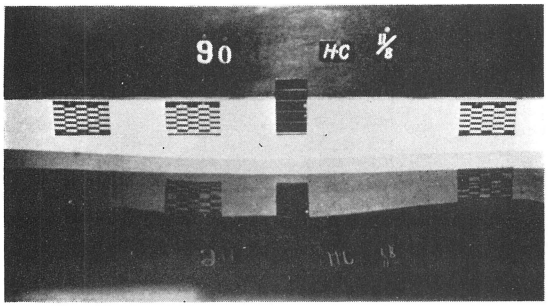

Photo. 7. Photograph of wave profile.

4. 1 Circular Cylinder

Fig. 6 (a) shows the result of the experiment on the semi-circular one. When the amplitude was small the value $\bar{A}$ by the experiment showed fair coincidence with the Ursell's one. But with the increase of the amplitude the value $\bar{A}$ got a slight less value on the average at large $\bar{\xi}_0$.

Now let us turn to investigate on the cylinder with segmental section, the

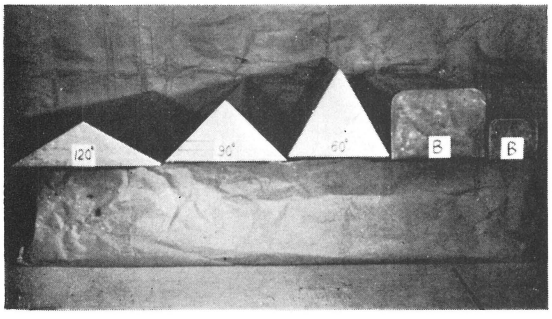

Photo. 8 (a) Cylinders.

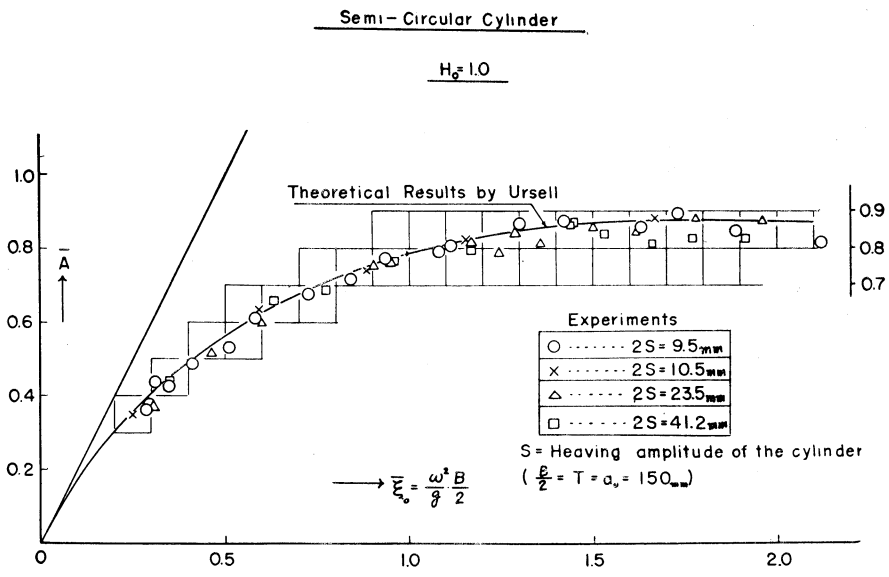

Fig. 6 a.

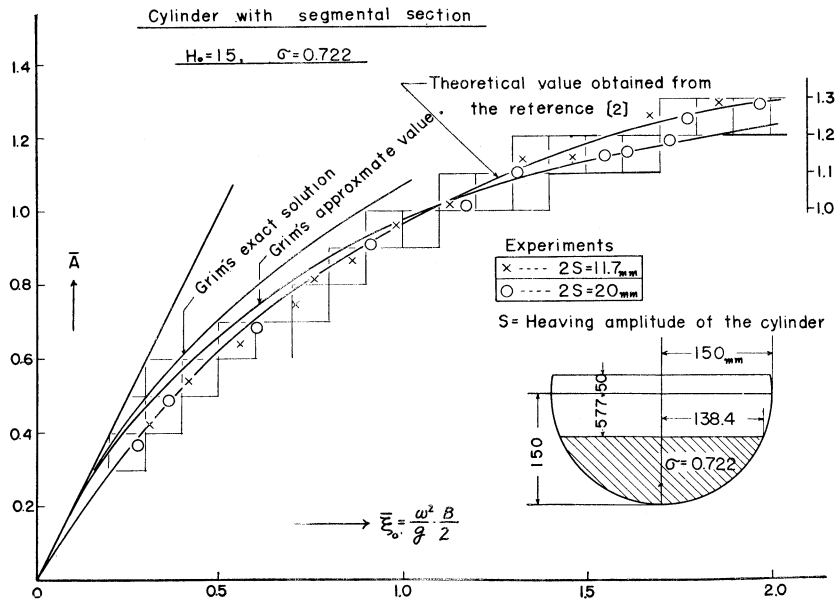

Fig. 6 b.

dimension of which being $T = 9.3$ cm, $\frac{B}{2} = 13.85$ cm, that is $\frac{B/2}{T} = H_0 = 1.5$, $\sigma =$ 0.722. The main results of the experiment could be summarized in Fig. 6 (b),

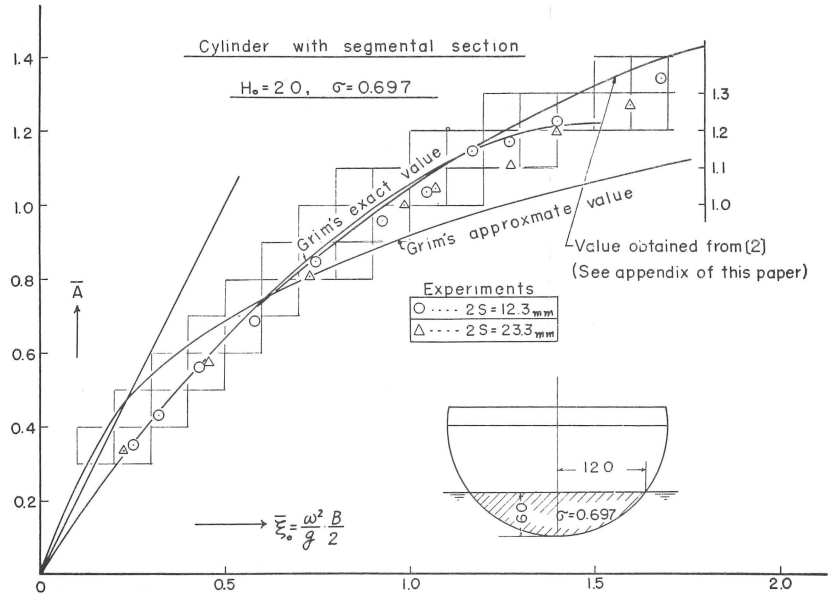

Fig. 6 c.

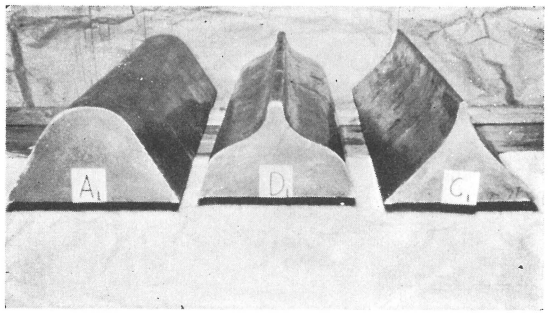

Photo. 8 (b) Cylinders.

which was much similar to the curve of $\bar{A}$ obtained from Fig. 7 of the author [2] by means of interpolation. The accurate value calculated by Grim [4] (Bild [7]) was too large. Approximate value was also too large at $\bar{\xi}_0 < 1.0$ but too small at $\bar{\xi}_0 > 1.0$. And it has been observed for this cylinder that the value $\bar{A}$ clearly got hump and hollow with the increase of $\bar{\xi}_0$. $\bar{\xi}_0$ which correspond to the hump or hollow varied with the amplitude of the plunger.

Next I should like to mention on Fig. 6 (c), which is the result of the experiment of the segmental section whose dimension is $T = 6.0$ cm, $\frac{B}{2} = 120$ cm, $H_0 = 2.0$, $\sigma = 0.697$. Exact value of Grim [4] correspond closely with the exprimental value, however the tendency of the curve varies with the increase of $\bar{\xi}_0$.

We have known from the experiment of the circular cylinder that the experimental value shows good coincidence with the Ursell's theoretical one. But a slight difference is found between the experimental value and the theoretical one, namely experimental value A has always undergone wavy variation with the increase of $\overline{\xi_0}$ and that the variation of the plunger-amplitude brings forth diversity of $\overline{\xi_0}$ for hump and hollow. It was also elucidated that the calculated value [2] was sufficient one for the segmental section.

4. 2 Triangular Clylinder

Experiment was done on the three cylinders with the apex angles of which were $\alpha = 60°$, $90°$, $120°$, namely $H_0 = 0.5774$, 1.0 and 1.732 respectively. Whereas σ was 0.5 for each cylinder. The values of H_0 and σ has been always constant in spite of the variation of the plunger-amplitude during the experiment. Fig. 7 (a), 7 (b) and 7 (c) indicate these results. Now let us consider of the cylinders

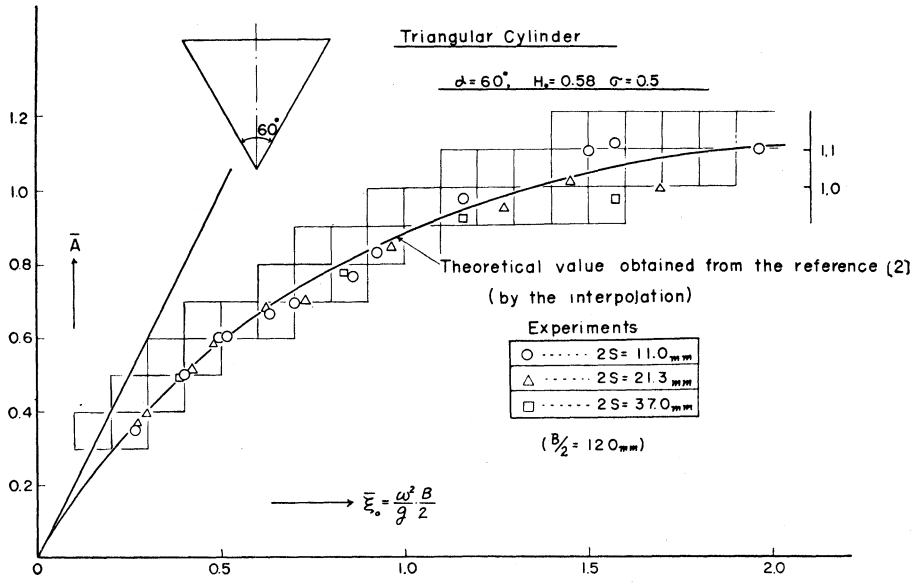

Fig. 7 (a).

$\alpha = 60°$ and $\alpha = 90$. Great hump and hollow was found at large $\overline{\xi_0}$, though the variation of the curve $\bar{A}$ by the amplitude of the plunger was small. These prismatic cylinders were non-wall-sided on the water line, but each of them had the angle of inclination, $\frac{\pi}{2} - \frac{\alpha}{2}$, respectively. In this case $\bar{A}$ might generally differs from that of Lewis form of wall-sided. This is called Wedge Effect in this report. On the value $\bar{A}$ of certain section there is generally found a difference between the experimental measurement and theoretical calculation, which is as follows:

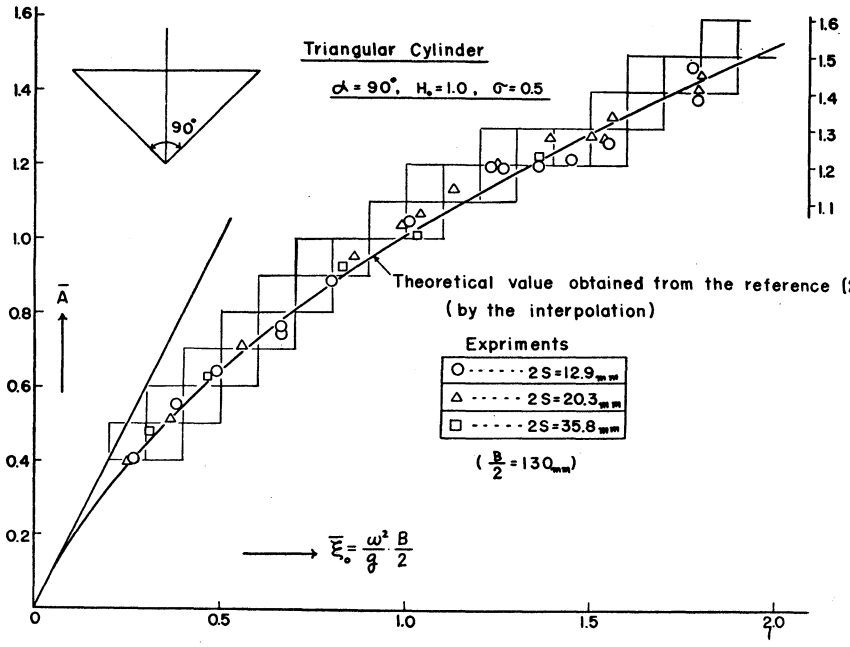
Triangular Cylinder
α = 90°, H₀ = 1.0, σ = 0.5
90°
Theoretical value obtained from the reference (2)
(by the interpolation)
Expriments
○ ------ 2S = 12.9 mm
△ ----- 2S = 20.3 mm
□ ----- 2S = 35.8 mm
(B/2 = 130 mm)
Ā
ξ̄₀ = ω²/g · B/2
0
0.5
1.0
1.5
2.0
0.2
0.4
0.6
0.8
1.0
1.2
1.4
1.6
1.1
1.3
1.5

Fig. 7 (b).

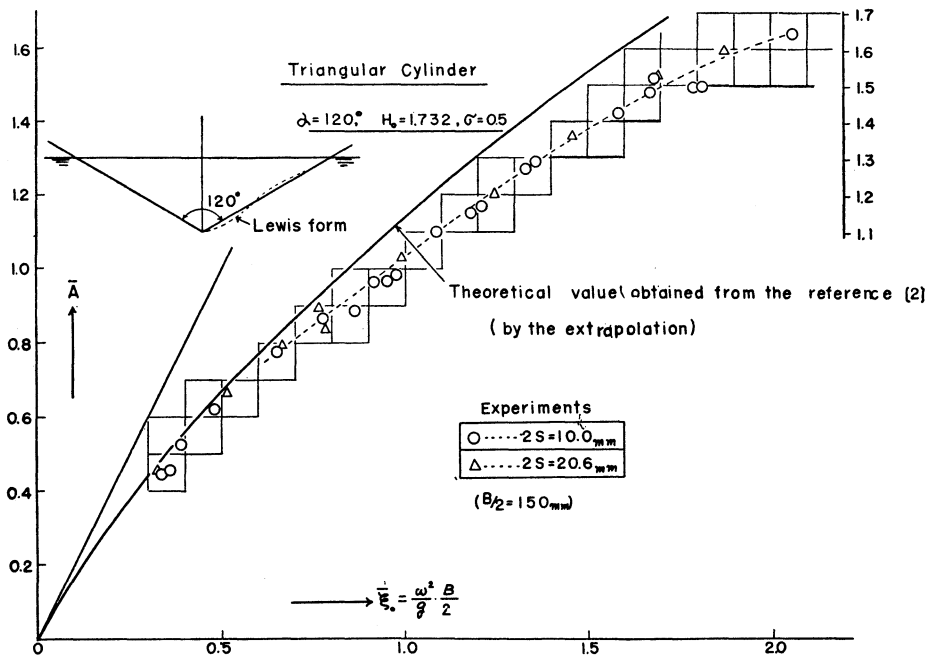
Triangular Cylinder
α = 120°, H₀ = 1.732, σ = 0.5
120°
Lewis form
Theoretical value obtained from the reference (2)
(by the extrapolation)
Experiments
○ ----- 2S = 10.0 mm
△ ----- 2S = 20.6 mm
(B/2 = 150 mm)
Ā
ξ̄₀ = ω²/g · B/2
0
0.5
1.0
1.5
2.0
0.2
0.4
0.6
0.8
1.0
1.2
1.4
1.6
1.1
1.3
1.5
1.7

Fig. 7 (c).

(1) Inadequacy of the linear theory when the steepness of the generated waves are large.
(2) Wedge effect
(3) Influence of the large amplitude of the plunger
(4) Variation of the section contour from the Lewis form in spite of the same H_0 and σ.

Steepness of the generated wave was $\beta = \frac{2\eta}{\lambda} = \bar{A} \cdot \bar{\xi}_0 \frac{S}{\pi \frac{B}{2}}$. Then $\beta \leqq 0.075$ was in case $\alpha = 90°$. When $\alpha = 60°$ and $\alpha = 90°$, the value $\bar{A}$ obtained from [2] by the interporation of H_0 and σ correspond closely with the experimental value. Then the item (1), (3), (4) and Wedge effect was assumed to be small. Next examine the case $\alpha = 120°$. Known from 7 (C), the theoretical curve of [2] was coincide with experimental one till $\bar{\xi}_0 \fallingdotseq 0.3$. And then experimental one decreased about 10% to 15% with the increase of $\bar{\xi}_0$. This was resulted from Wedge effect that had a little influence at small $\bar{\xi}_0$ but the effect increased gradually with the increase of $\bar{\xi}_0$. It is also important that the Wedge effect gives less value than the theoretical one obtained from [2] for the same H_0 and σ.

4. 3 Rectangular cylinder with rounded corner

Experiment was held on the four sections of $H_0 = 1.0$, 1.25, 1.5 and 2.0, changing the draught of the cylinder with rounded corner which radius of curvature $r = 46$ mm.

The value σ was 0.98, 0.975, 0.97 and 0.96 respectively. For the small ξ_0 we used

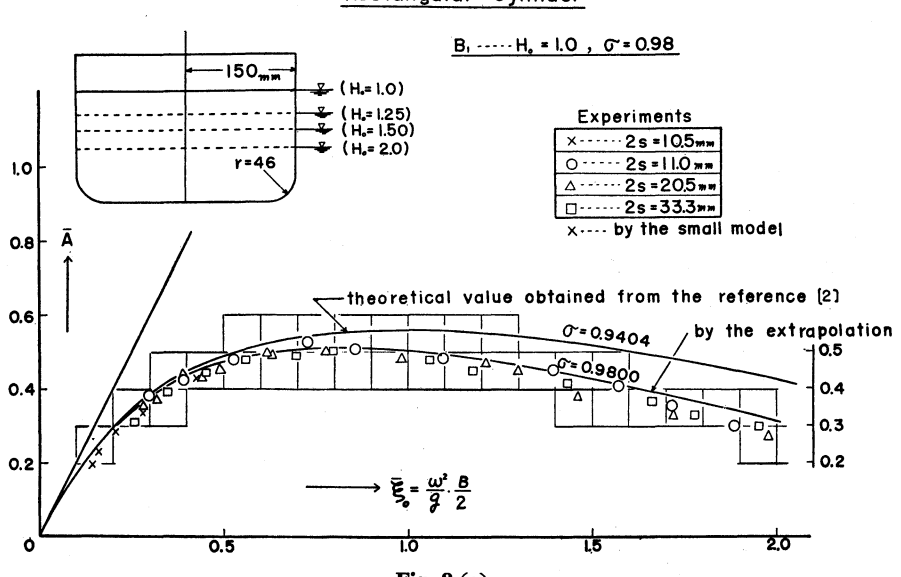

Fig. 8 (a).

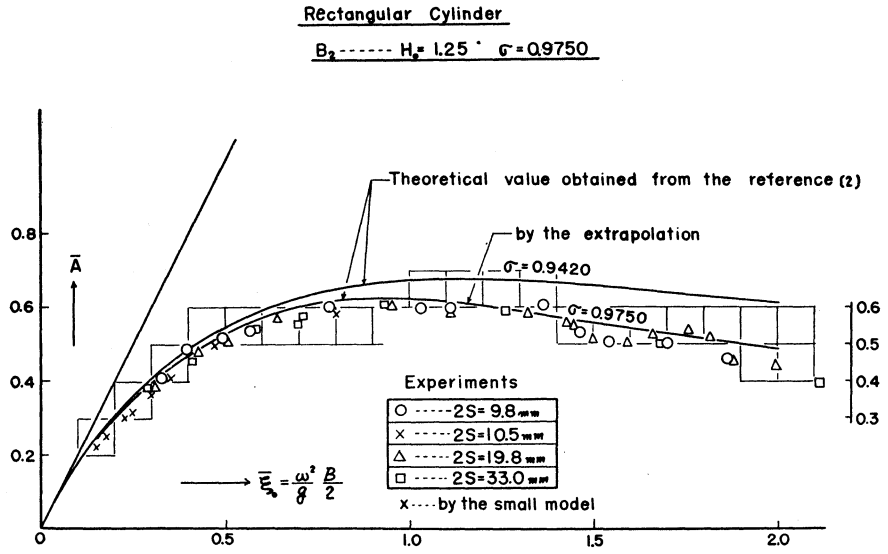

Fig. 8 (b).

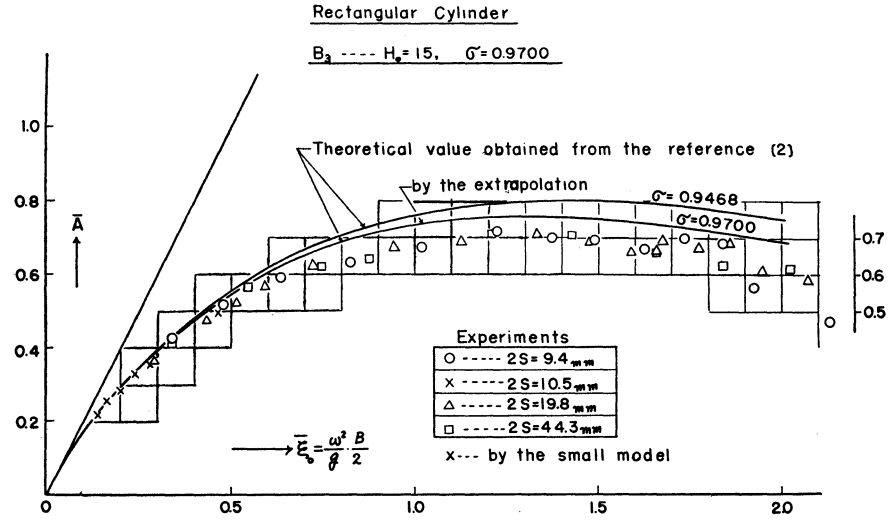

Fig. 8 (c).

a similar model of ½ scale, to take off the influence the shallow water effect. These cylinders are of course wall-sided. Fig. 8 (a), 8 (b), 8 (c) and 8 (d) show the results of the test.

On the cylinders B_1 and B_2, the theoretical one obtained from [2] by extrapolation corresponds closely to the experimental one generally. But as the case of the circular cylinder, the experimental value slightly decreases with the increase

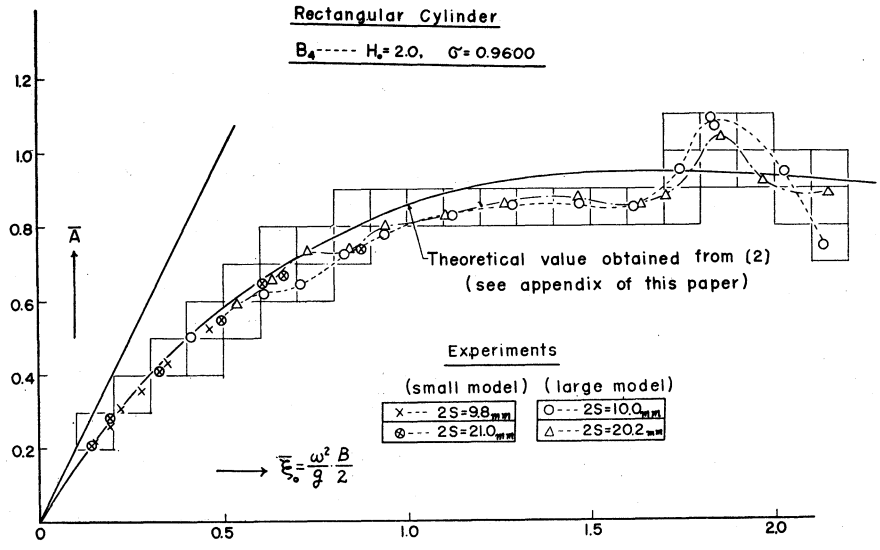

Fig. 8 (d).

of $\bar{\xi}_0$. In regard to the cylinder B_3 the experimental value decreased abut 5~10% at $\bar{\xi}_0>0.5$. And hump and hollow were observed clearly in case of B_2 and B_3. H. Holstein [3] also pointed out the phenomena that the minimum and maximum were observed in the experiment for the rectangular cylinder. In the experiment of B_4 very large hump was found at $\bar{\xi}_0 \fallingdotseq 1.85$. And yet I should like append the value $\bar{A}$ and K_4 for $H_0=2.0$ of Lewis form in the appendix [II].

4. 4 Cylinder A

This cylinder has the section which is similar to that found at the rear of the ship, which is given in Fig. 9 (a). As the figure indicates, cylinder A_1 was designed to be used also as Cylinder A_2 by adding the projecting part under the water surface. Then experiment was done by varying the draught in three ways: A_1–W_1, A_1–W_2 for the cyinder A_1, and A_2–W_1, A_2–W_2 for the cylinder A_2 respectively.

Both A_1, A_2 have the same $H_0=1.0$ on the water line W_1 and the same $H_0=1.25$ on W_2. The condition of the test being non-wall sided either, A_1–W_1 and A_2–W_1 had the inclination of 60° which is the same condition with the prismatic cylinder of $\alpha=60°$. So that Wedge Effect was assumed to be small. Figure 10 (a), 10 (b) show the result.

Either of them had great hump and hollow $\bar{A}$ at $\bar{\xi}_0>1.0$. And also it was manifested that the value of $\bar{\xi}_0$ which correspond to the hump and hollow was varied with the amplitude of plunger. On the section A_1–W_1 the theoretical value agreed quite well with the average value of the experimental one, while on the section A_2–W_1 the theoretical one was less than the experimental one by 19~20%.

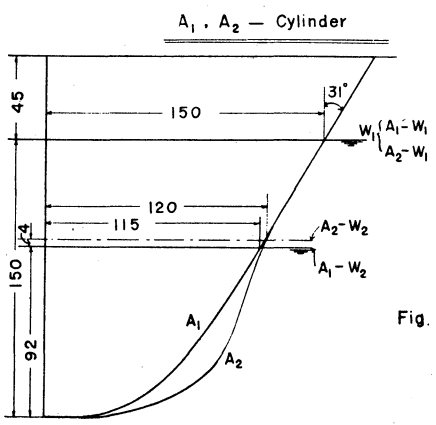

Fig. 9(a)

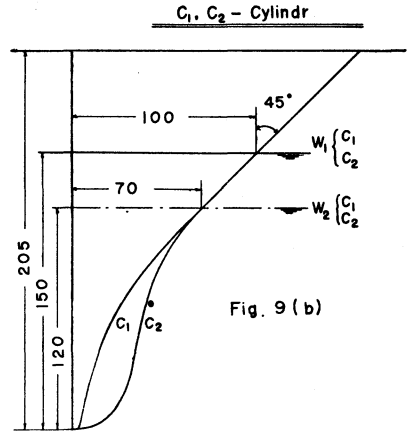

Fig. 9 (b)

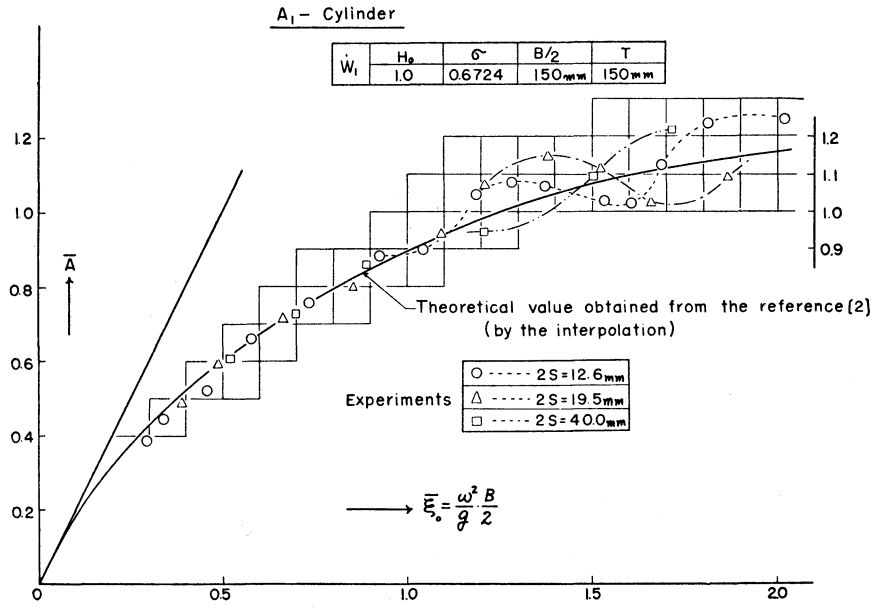

Fig. 10 (a).

The value σ of A_2 was larger than that of A_1, therfore $\bar{A}$ obtained from the calculation [2] was smaller than that of A_1. The section A_2–W_1, however, took greater variation of section contour from Lewis form rather than A_1–W_1 and paticurally nearby the water line it varied finely and at the lower part fully.

For this reason when the value $\bar{\xi}_0$ becomes large, that is, as the progressive wave length decreases, the upper part of the plunger near the water line exerted greater influence on the value $\bar{A}$ than the lower part. This is why the experimen-

tal value is larger than the theoretical one. It is most probable that the section A_2–W_1 gets large $\bar{A}$ not for the Wedge effect but for the variation of the section coutour from the Lewis form.

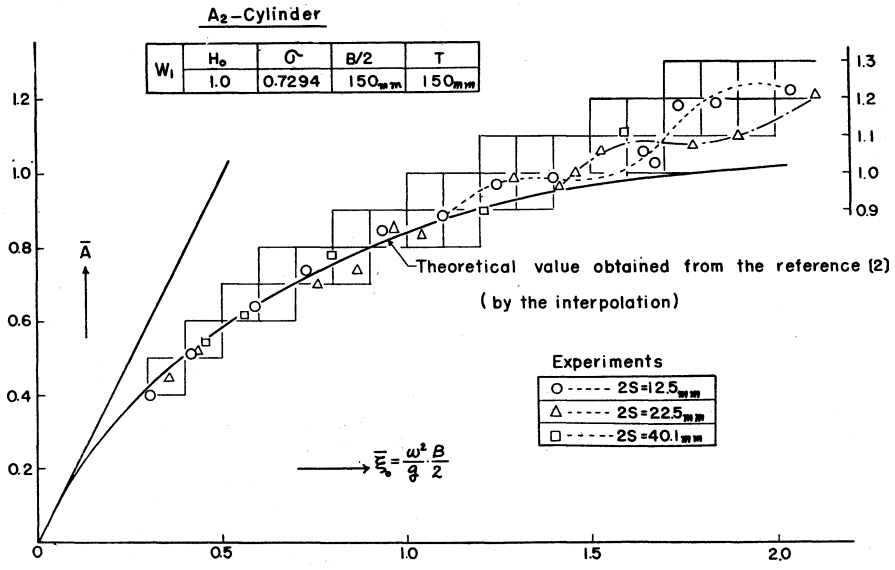

Fig. 10 (b).

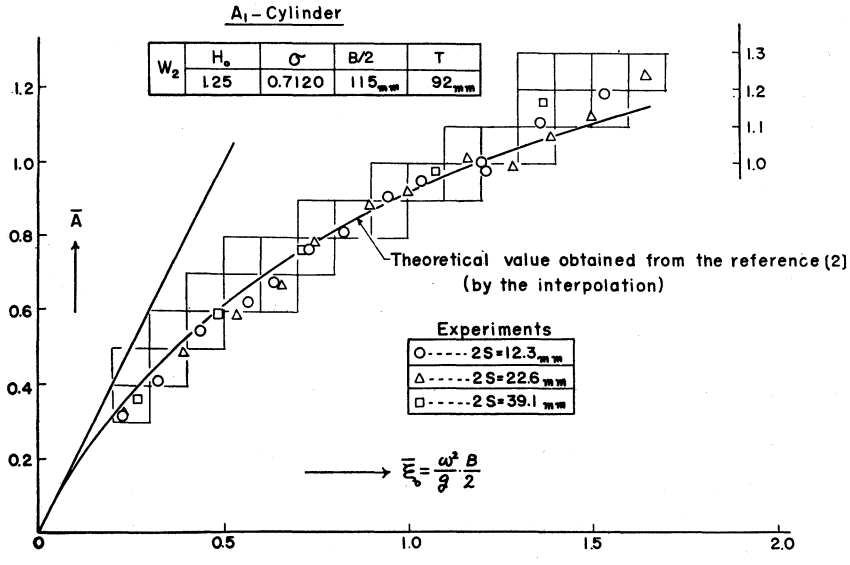

Fig. 10 (c).

Now compare the cases of $A_1 - W_2$ and $A_2 - W_2$ which is shown in Fig. 10 (c), 10(d). Generally both experimental and theoretical ones correspond closely

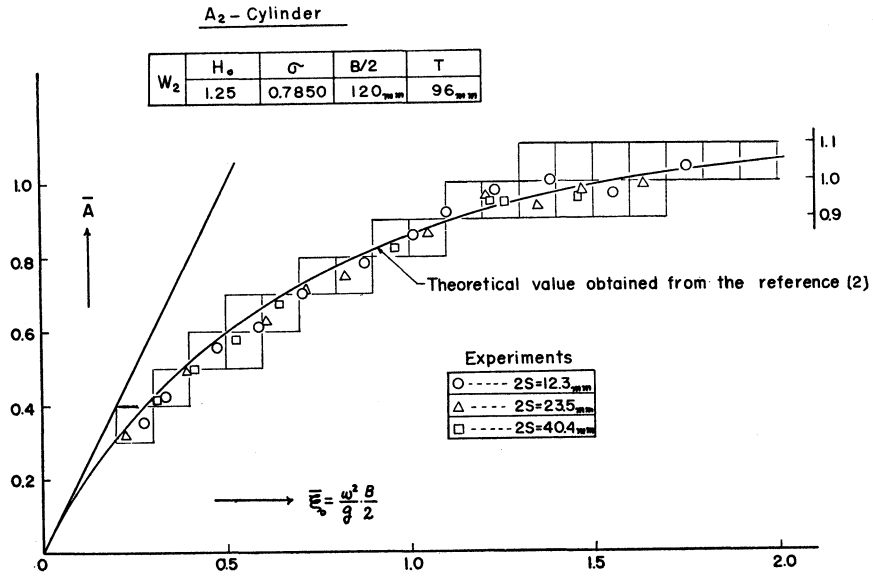

Fig. 10 (d).

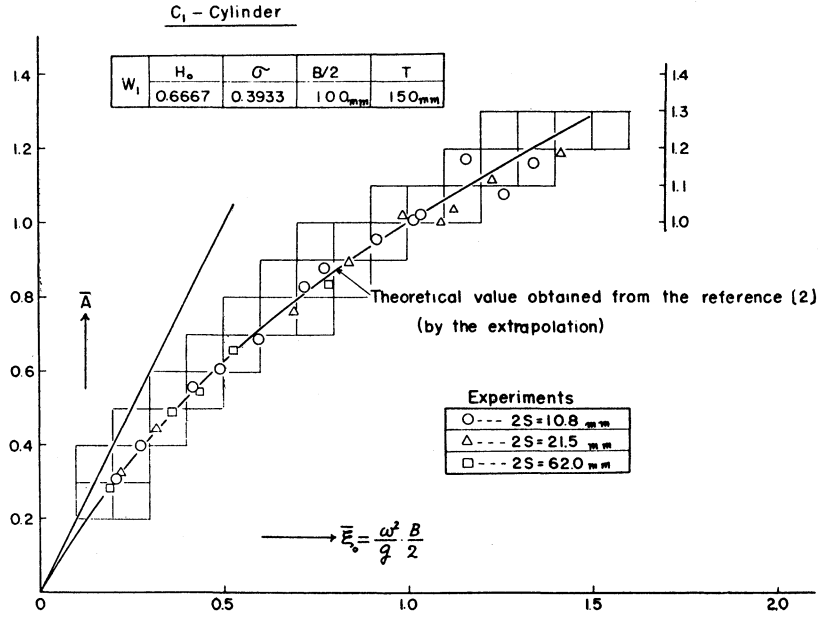

Fig. 11 (a).

in each cases. On the section $A_1 - W_2$ the experimental one was a little larger at $\xi_0 > 1.2$ under the influence of the variation of the section contour from Lewis form. While the section $A_2 - W_2$, being closely resembles to the ellipes $H_0 = 1.25$, both theoretical and experimental ones agreed quite well.

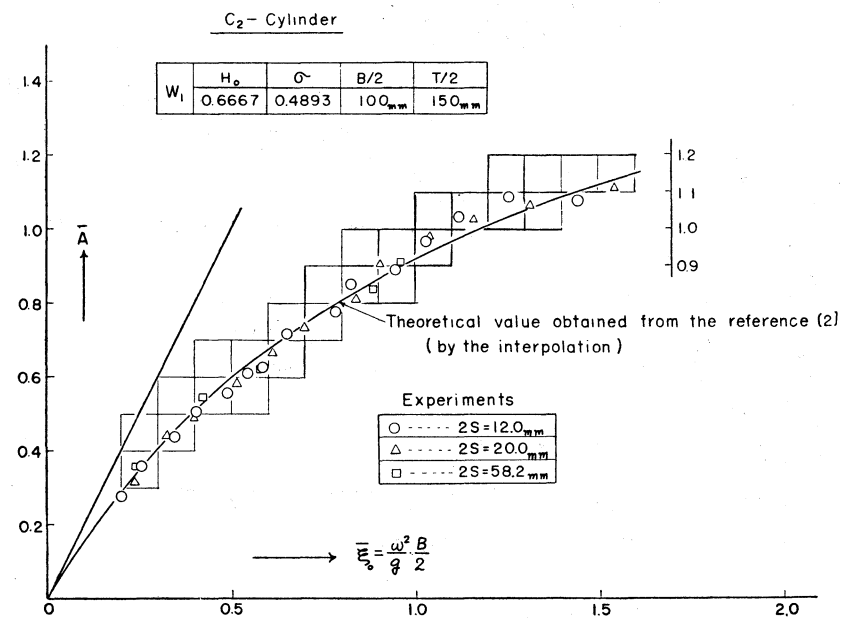

Fig. 11 (b).

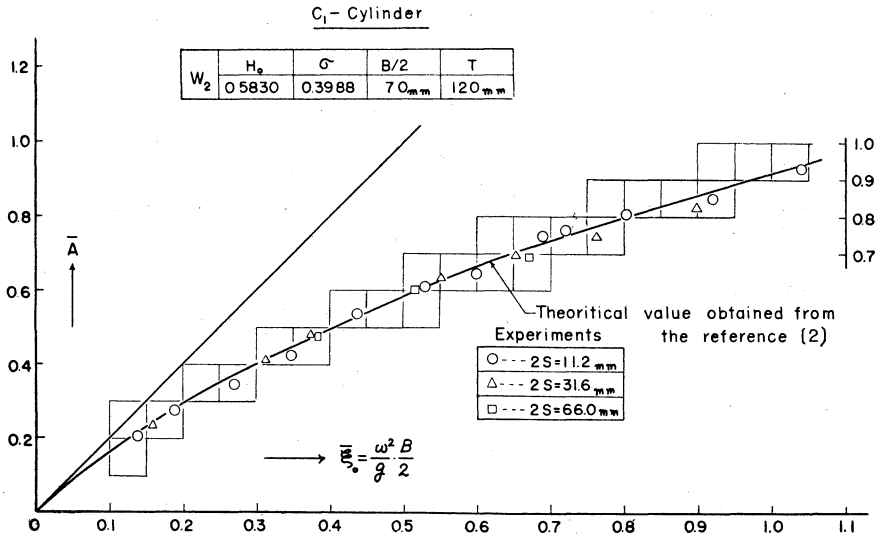

Fig. 11 (c).

4. 5 Cylinder *C*

The section of this cylinder is similar to that of a ship's fore and after part. (See Fig. 9 (*b*)). Section C_2 was the one which was swelled under part of C_1. Draught was varied by two times, W_1 and W_2. The section $C_1 - W_1$ and $C_2 - W_1$ has same $H_0 = \frac{2}{3}$ and $\sigma = 0.3933$ and 0.4893 respectively. Also $\sigma = 0.3988$ and 0.5690 on each section $C_2 - W_1$ and $C_2 - W_2$ (in this case $H_0 = 0.583$). Fig. 11 (a), (b), (c), (d) show these results. On the water line W_1 and W_2 the sections C_1 and C_2 had an inclination of 45°, the Wedge effect was, however, supposed to be small judging from the experimental results of trianglar cylinder of $\alpha = 90°$. These experimental value showed hump and hollow, while theoretical value agreed quite well with the average one of the experiment. The experiment was done at the large amplitude $2S \fallingdotseq 70$ mm, in due consideration of the pitching of the ship. But no visible variation was found on the average value of $\bar{A}$.

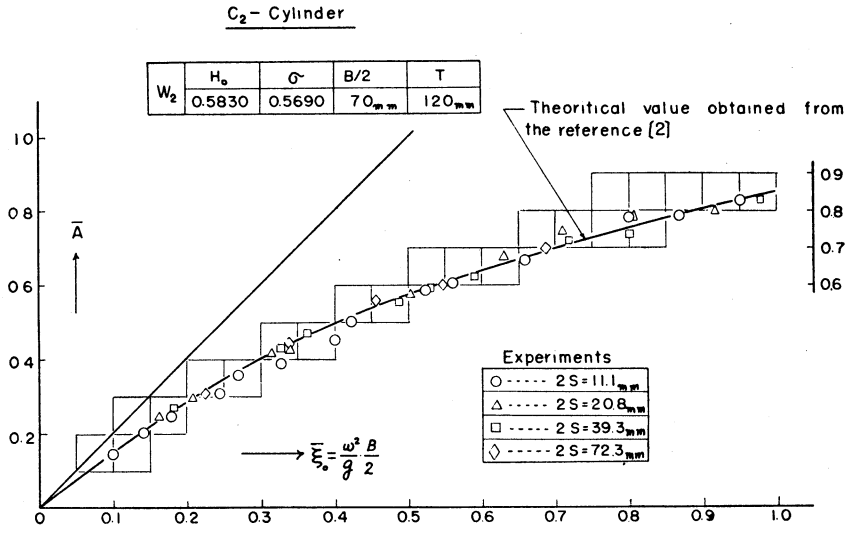

Fig. 11 (d).

4. 6 Cylinder *D*

For the eight ship models K. Kroukovsky [5] had made calculation of coupled oscillation of heaving and pitching by Strip Method. And had compared it with the experimental one. Then he said that the theoretical calculation had failed for the Yacht-model 1699 *B*, 1699 *D* and concluded that Strip Method was inadequate for these type. The fact is that the amplitude of heaving and pitching obtained from theoretical calculation is too small. These yacht-shaped model has fine section and sloping sides at the water line. K. Kroukovsky [5] calculated the damping force from Grim [4]. However Grim [4] had large error for

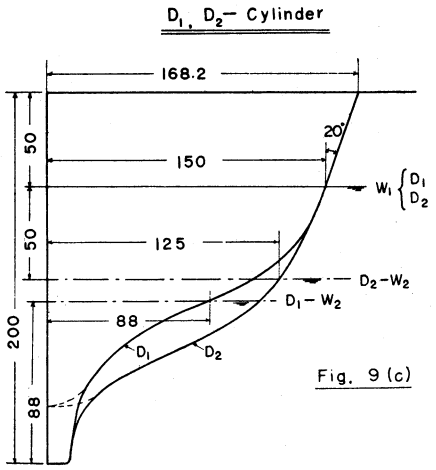

Fig. 9 (c)

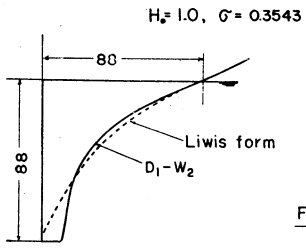

Fig. 9 (d)

the fine sections, which was alluded to by the auther in [2]. It is supposed that the failure of the calculation for the yacht-model was mainly due to the damping force obtained from Grim [4] being too large. Then the author took the measurement of $\bar{A}$ on the cylinder D whose section was similar to the midship section of the yach-model. Fig. 9 (C) indicate the section of the cylinder. D_2 was the one which was swelled the under part of D_1. $D_1 - W_1$, $D_2 - W_1$ was $H_0 = 1.0$ and

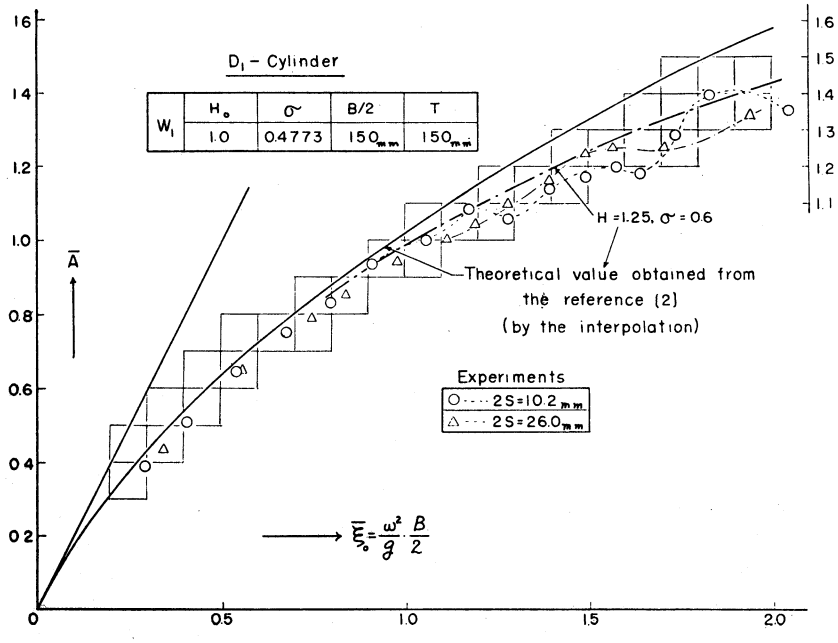

Fig. 12 (a).

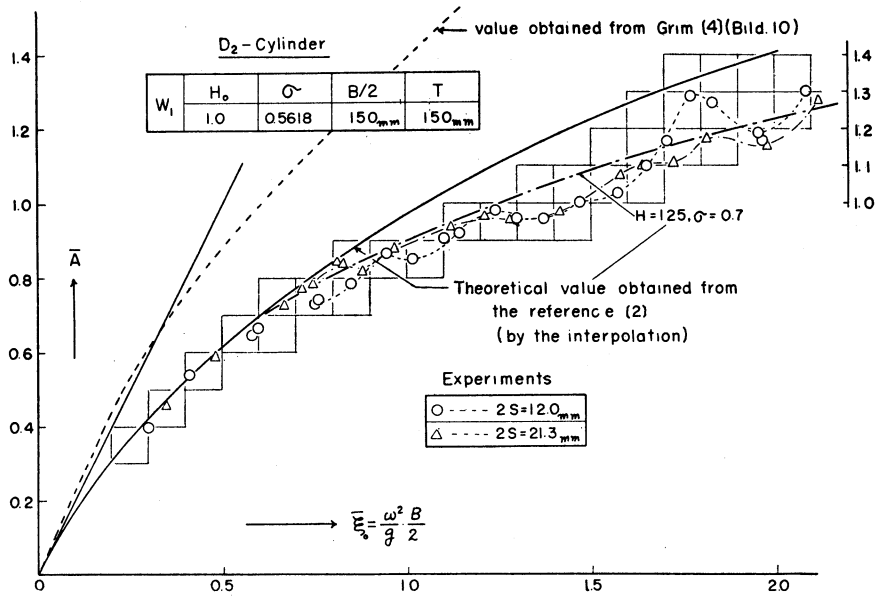

Fig. 12 (b).

$\sigma = 0.4773$ and 0.5618 respectively. Fig. 12 (a), (b) indicate the results of the test. In the range of $\bar{\xi}_0 < 0.8$, the value of $\bar{A}$ obtained by the experiments corresponds closely with the theoretical one obtained from [2] but hump and hollow was generally observed at $\bar{\xi}_0 > 0.8$. On the $D_2 - W_1$, especially, the large hump was found at $\bar{\xi}_0 \fallingdotseq 1.8$.

In fig. 12 (b) we inserted for reference the value obtained from Abb. 10 of Grim [4] by interporation of σ. The values are very large, especially in the case $D_1 - W_1$ they are too large to be drawn in the figure. The average value of the experimental one is smaller than the theoretical one at $\bar{\xi}_0 > 0.8$. Principal cause for this is supposed as follows: The angle of inclination being about 80° Wedge effect would be supposed to be negligible. The section contur of $D_1 - W_1$ and $D_2 - W_1$ vary from the Lewis form, especially fully near about the water line and finely about the lower part. These were just against the case of $A_2 - W_1$. That is, the larger become the value $\bar{\xi}_0$, the more great influence exert the upper part on the value $\bar{A}$. Therfore the experimental curve is lower than the theoretical one. When $\bar{\xi}_0$ is large, namely when the produced wave-length is small, the lower part of the cylinder do not exert any influence on the wave-making.

Then let us discuss on the section without the small swelling part of the lower part. If the section is showed by the dotted line in Fig. 9 (c), the section $D_1 - W_1$ takes $H_0 = 1.25$ and $\sigma \fallingdotseq 0.6$, $D_2 - W_1$ takes $H_0 = 1.25$ $\sigma \fallingdotseq 0.7$. The value $\bar{A}$ calculated from [2] for that H_0 and σ resulted in approximate quantity to the experimental value as was illustrated by the chain line in Fig. 12 (a), (b).

On the section $D_1 - W_2$ the experimental value is genrally lower than the

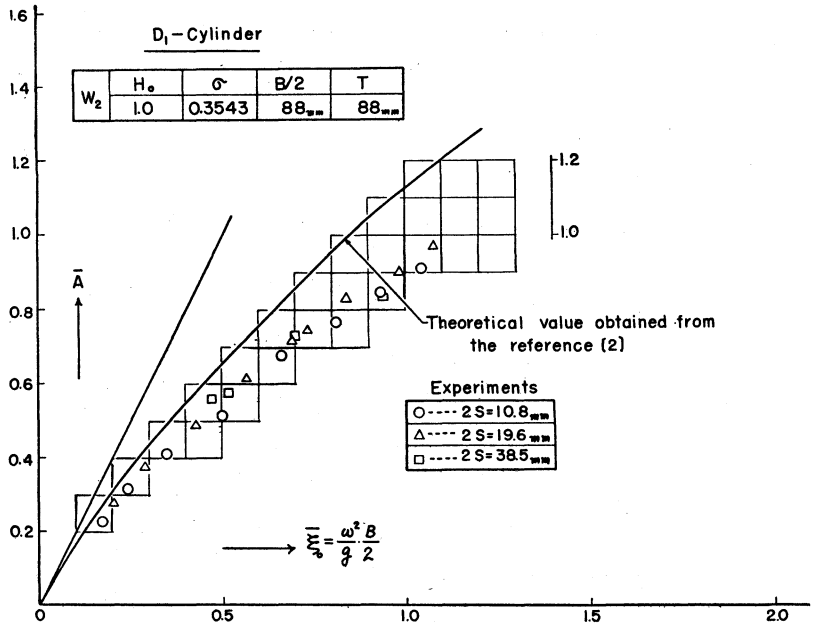

Fig. 12 (c).

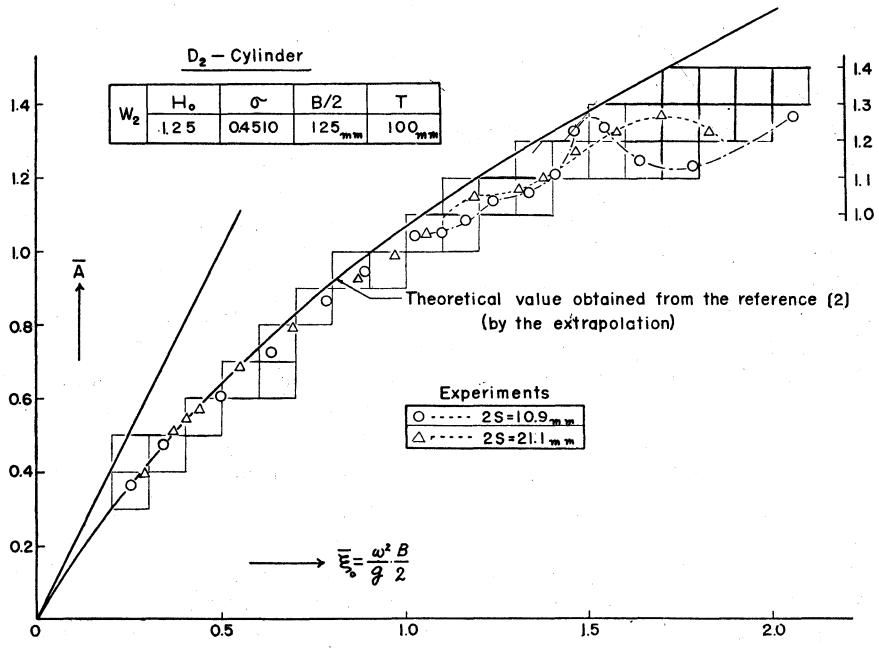

Fig. 12 (d).

theoretical one as was shown in Fig. 12 (c). The decreasing percentage from the theoretical value of $\bar{A}$ is remarkable with the increase of $\bar{\xi}_0$, namely, 13 % at $\bar{\xi}=0.4$, 16 % at $\bar{\xi}_0=0.7$ and 20 % at $\bar{\xi}_0=1.0$. This section contour varies finely at the upper part and fully at lower part from Lewis form (See Fig. 9 (d)).

If we judge from this view point experimental quantity is assumed to be slightly larger than the theoretical one. However, actually reverse is the case. This is owing to the Wedge effect. The inclination on the water line was about 26° which corresponds to the prismatic cylinder of $\alpha=128°$. Then it is supposed that the experimental value became lower owing to the Wedge effect which is larger than the case $\alpha=120°$. The next one, D_2-W_2, the experimental value of $\bar{A}$ was lower than the theoretical one from the same cause as D_2-W_1. We denote the angle of inclination of the section contour on the water line by θ. When θ is small, the Wedge Effect correction are obtained approximately from the experiments of this paper. It is shown in Fig. 13. On the other hand, the influence of the variation from the Lewis form such as A_1-W_1, D_1-W_1, D_2-W_1 could not be formalized. For a certain cylineder, however, concidence between the experimental $\bar{A}$ and theoretical one could be abtained, if we calculated it by taking many terms of ζ in the equation (4) of [2] and using the mathemetical representation more approximate to the section of the cylinder. But really for the section which has great displacement from Lewis from, we could correct the value obtained from the equation [2], taking into consideration the experimental result in this paper.

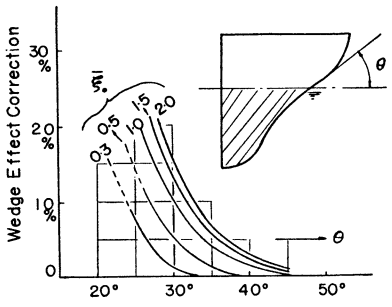

Fig. 13.

6. Conclusion

We could gain the following conclusion within the limit $\bar{\xi}_0<2.0$ from the results above-mentioned.

(1) An sufficient average quantity was given by the theoretical calculation of F. Ursell [1] and the author [2] for the progressive wave height generated by the forced heaving of the cylinders whose section was semicircular and resemble to that of Lewis form.

(2) The $\bar{A}$ of the measurements give rise to hump and hollow, especially with the increase of $\bar{\xi}_0$ they becomes greater.

(3) In this experiment the influence of the amplitude of plunger over the value $\bar{A}$ was generally small. But great influence was exerted over the $\bar{\xi}_0$ at which hump and hollow was forced to be generated in the case of high heaving frequency.

(4) Judging from the test of triangular cylinder and so on, Wedge Effect was

small till the inclination of the section contour on the water line getting 45°. So the calculation of [2] was good for the cylinders above-mentioned. Wedge Effect however came to be large in the case $\alpha = 120°$ and V-type section opened widely as the section $D_1 - W_2$.

(5) Owing to Wedge Effect the experimental value was lower than the theoretical one [2] for the same σ and H_0. Paticulally the tendednecy was remarkable with the increase of $\bar{\xi}_0$.

(6) The different $\bar{A}$ from the calculated value of [2] was found at large ξ_0 when the variation from Lewis form was conspicuous, even if H_0 and σ are the same ones respectively. The fact that $\bar{A}$ was higher or not than the theoretical one corresponded to whether the upper part of the section under the water line changed finely or fully from the Lewis from.

(7) Wedge Effect and the influence of displacement from the Lewis form was small at the points where $\bar{\xi}_0$ was small.

(8) We can compute from [2] the wave producing paticularity of plunger type wave making machine.

My grateful thanks are due to Dr. Y. Watanabe and to Professor M. Kurihara for the helpful opinions on my research. I am especially indebted to Mr. Awaya for considerable assistance in the preparation for recording apparatus and to Mr. Ikeda and Mr. Inoue for the helful cooperation in the preparation of the driving apparatus.

My debt to Mr. Arakawa for his unfailing effort and assistance at all stages of this research cannot be adequately expressed.

List of Reference

]1] F. Ursell ..... Quart. J. Mech. Appl. Math. (1949, p. 18)
[2] F. Tasai ..... J. of the Society of Naval Architects. Japan
[3] H. Holstein ..... W. R. H. Dec. (1936); s. 375-389
[4] O. Grim ..... Jahrb. Schiff. Tech. Ges. (1953)
[5] K. Kroukovsky ..... S. N. A. M. E (1957)
[6] F. M. Lewis ..... S. N. A. M. E (1929)
[7] C. Taniguchi, M. Shibata ..... Seibu-Zoesenkai-Kaiho no. 9 (1954)

APPENDIX

[1] Paticurality of the Measuring Float

1. Heaving Equation of the float and its solution

Heaving motion of the float is supposed two-dimensional because of the float being slender. Fig. 14 shows the section of the float, in which x is taken along the horizontal axis, y along the vertical axis and z-axis is taken right-angled with the paper. The symbol $W-W$ denotes the two-dimensional wave towards x-direction. Half width of the float, in the figure, is denoted by a, draught by T

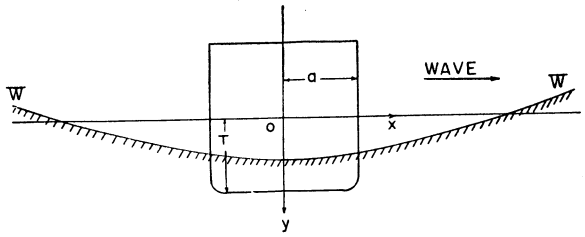

Fig. 14.

and length towards z-direction by l. Then put r_m the amplitude of the surface wave, the isobars are given by

$$\eta_w = r_m e^{-k_0 y} \cos(k_0 x - \omega t) \cdots\cdots (1)$$

where ω = wave circular frequency.

In practically $a = 1$ cm and wave length used for the experiment is $\lambda > 40$ cm so that resulted into $a/\lambda < 0.025$. Therefore external force by the wave is obtained accurately by putting $x = 0$ into the equation (1).

The followings are the symbols used in this paper.

y = heaving displacement, V_0 = displacement volume of the float

A = water plane area $= 2al$

σ = sectional area coefficient $= \dfrac{S_w}{2aT}$, $H_0 = \dfrac{a}{T}$

S_w = immersed sectional area of the float

M_0 = heaving mass of the float

m' = Equivalent mass of the pen P_1, $M = M_0 + m'$

ΔM = added mass of the float, α_0 = added mass coefficient $= \dfrac{\Delta M}{\rho V_0}$

ξ_0 = heaving parameter of the float $= \dfrac{\omega^2}{g} a$

N = damping coefficient, Fy = wave force

k_s = spring constant of S_1 (Fig. 4)

ΔE = dynamical change of the wire tension

Now the equation of heaving motion of the float is expressed as follows:

$$M_0 \frac{d^2y}{dt^2} + \Delta M \frac{d^2}{dt^2}(y - \eta_{w_0}) + N \frac{d}{dt}(y - \eta_{w_0}) + \rho g A y = F_y - \Delta E \cdots\cdots (2)$$

(η_{w_0} denote the value η_w at $x = 0$)

If movement of the pen were taken into consideration

$$\Delta E = m' \frac{d^2y}{dt^2} + k_s y \cdots\cdots (3)$$

is obtained. In case ΔE be eliminated from the equation (2) and (3), and using

$M_0 + m' = M$ the following equation would be given.

$$M\frac{d^2y}{dt^2} + \Delta M\frac{d^2}{dt^2}(y-\eta_{w_0}) + N\frac{d}{dt}(y-\eta_{w_0}) + (\rho gA + k_s)y = F_y \cdots\cdots(4)$$

In this equation y indicates displacement from the equilibrium condition where the wire is suffered from the statical tension $E_0 \doteqdot 2$gr.

The whole tension of the wire E is written as

$$E = E_0 + m'\frac{d^2y}{dt^2} + k_s y \cdots\cdots(5)$$

Fy and N are given as follows:

$$Fy = \rho g \gamma_m \cdot A \cdot e^{-k_0 T}\cos\omega t \cdots\cdots(6)$$

$$N = \int_0^l \frac{\rho g^2}{\omega^3}\cdot\bar{A}^2\cdot dz = \frac{\rho g^2}{\omega^3}\cdot\bar{A}^2 l \cdots\cdots(7)$$

$$\text{Put}\quad \frac{\rho gA + k_s}{M+\Delta M} = \nu_0^2,\ 2h = \frac{N}{M+\Delta M},\ \Delta M = \rho V_0\alpha_0, \cdots\cdots(8)$$

we have $\dfrac{\Delta M}{M+\Delta M}\cdot\dfrac{\omega^2}{\nu_0^2} = \dfrac{\xi_0}{H_0}\cdot\sigma\alpha_0$. Therefore the equation (5) reduces to

$$\ddot{y} + 2h\dot{y} + \nu_0^2 y = f_1\cos\omega t - f_2\sin\omega t \cdots\cdots(8)$$

where

$$f_1 = \nu_0^2\cdot\gamma_m\cdot e^{-\frac{\xi_0}{H_0}}\left(1 - \frac{\xi_0}{H_0}\cdot\sigma\cdot\alpha_0\right)$$

$$f_2 = 2h\gamma_m\cdot\omega\cdot e^{-\frac{\xi_0}{H_0}}$$

Let

$$y = b\cos(\omega t - \varepsilon) \cdots\cdots(9)$$

denote the forced heaving displacement of the float, we obtain

$$b = \frac{\sqrt{f_1^2 + f_2^2}}{\sqrt{(\nu_0-\omega^2)^2 + 4h^2\omega^2}}$$

and put

$$\Lambda = \frac{\omega}{\nu_0},\quad \kappa = \frac{2h}{\nu_0},\quad f_0 = e^{-\frac{\xi_0}{H_0}},\quad f_\alpha = 1 - \frac{\xi_0}{H_0}\sigma\alpha_0$$

$$f_A = \kappa\Lambda \cdots\cdots(10)$$

then it reduces to

$$b = \frac{\gamma_m\cdot f_0\cdot\sqrt{f_\alpha^2 + f_A^2}}{\sqrt{(1-\Lambda^2)^2 + f_A^2}} \cdots\cdots(11)$$

Therefore magnification factor of the heaving amplitude $Y = \dfrac{b}{\gamma_m}$ is given as follows:

$$Y = \mu\cdot f_0\cdot\sqrt{f_\alpha^2 + f_A^2} \cdots\cdots(12)$$

where $$\frac{1}{\mu} = \sqrt{(1-A^2)^2 + f_A^2}$$

Now, $$f_A = \kappa A = \frac{2h\omega}{\nu_0^2} = \frac{N\omega}{\rho g A + k_s}$$

As the k_s being small, regarding as $k_s \fallingdotseq 0$, the equation

$$f_A = \frac{N\omega}{\rho g A + k_s} \fallingdotseq \frac{\bar{A}^2}{2\xi_0} \quad \cdots\cdots(13)$$

is obtained.

Phase lag ε is given by the equation

$$\varepsilon = \tan^{-1}\left\{ \frac{\frac{\kappa A}{1-A^2} - \frac{f_A}{f_\alpha}}{1 + \frac{\kappa A}{1-A^2} \cdot \frac{f_A}{f_\alpha}} \right\} \quad \cdots\cdots(14)$$

The wire tension E should always be positive in order to operate the wave measuring apparatus on the above mentioned condition, namely

$$E_0 + m' \frac{d^2y}{dt^2} + k_s \cdot y > 0$$

therefore next equation is given

$$E_0 > \left| m' \frac{d^2y}{dt^2} + k_s y \right| \quad \cdots\cdots(15)$$

2. Free heaving Period of the Float

It is observed from the free heaving experiment that the first one cycle shows complicated motion but since second one it damps with constant period. These constant period is denoted by T_n. Natural frequency of the heaving ν_0 is deduced from

$$\nu_0^2 \fallingdotseq \frac{\rho g A + k_s}{M + \rho V_0 \alpha_0}$$

α_0 is computed from [2]:

$$\alpha_0 = \frac{C_0 \cdot \frac{\rho \pi a^2}{2} \cdot l \cdot K_4}{\rho \cdot 2a\, T \cdot l \cdot \sigma} = \frac{C_0 \cdot \pi a}{4T\sigma} \cdot K_4 \quad \cdots\cdots(16)$$

For the section of this float, $C_0 \fallingdotseq 1.4$ is obtained from F. M. Lewis [6]. Then putting $V_0 = 25.4\,\text{cm}^3$, $T = 0.86\,\text{cm}$, $\sigma = 0.98$ $H_0 = 1.16$ and $a = 1\,\text{cm}$ into the equation (16) the following one

$$\alpha_0 = 1.305\ K_4 \cdots\cdots(17)$$

is given. Frame D_1 and D_2 exert the rotation, so that the equivalent mass have to be considered for the heaving of the float. Also taking the m' of the pen into consideration, $(M_0 + m')g = M.g \fallingdotseq 27\,\text{gr}$ is given. Being $k_s = 1.2\,\text{gr/cm}$ and $l = 15\,\text{cm}$,

$\xi_0 = \frac{v_0^2}{g}$ a is calculated by the next equation:

$$\xi_0 = \frac{\rho g\, 2a^2 l + k_s \cdot a}{Mg + \rho g V_0 \alpha_0} = \frac{30.2}{27 + 25.4 \times 1.305\, K_4} \quad \cdots\cdots\cdots\cdots\cdots\cdots (18)$$

The equation denotes the ralation between ξ_0 and K_4 which was obtained from the definition of the natural heaving frequency.

Since the second cycle, on the other hand, K_4 is given approximately as the function of ξ_0 by using the calculated value of [2] for the forced heaving, assuming that it is nearly close to the regular heaving condition. Fig. 15 shows

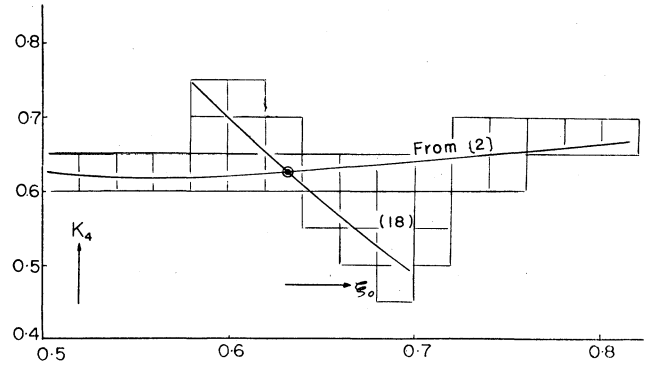

Fig. 15.

the equation (18) and the value of $K_4 - \xi_0$ obtained from [2]. From the intersecting point of these curves it is obtained $\xi_n = 0.633$ and $K_4 = 0.625$, and then $\nu_n = 24.9$, $T_n = 0.252$ sec could be obtained. Generally ν_n is approximately given by the above-mentioned method using the calculated value of [2] for the computation of the two-dimensional cylinders. T_n is resulted $0.25 \sim 0.26$ sec in the free heaving experiment of the wave measuring float.

3. Calculation of Y

Magnfication factor Y is computable from the equation (10) (12) and (13), if the paticulality of the float (H_0, σ, l, T, V_0), and circular frequency of the forced heaving ω are given.

Table. 2 illustrate Y and $Z = 1/Y$ for the 2.0, 1.5, 1.0 and 0.5 which are heaving parameter $\bar{\xi}_0 = \frac{\omega^2}{g} \cdot \frac{B}{2}$ of the wave-making circular cylinder. This is also given in Fig. 16. $\bar{\mu}$ in the table 2 denotes the heaving magnification factor used in the List of Reference [7].

That is, $\nu_0 = \nu_n = \text{const.}$ is put without computing it for each ω. And the constant value of f_A for ν_n are used on each frequency. In other words it is cal-

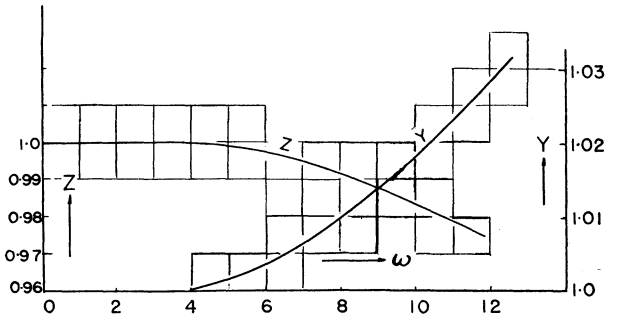

Fig. 16.

Table 2.

ω	11.43	9.9	8.1	5.7
$\hat{\xi}_0$	0.1333	0.1	0.0667	0.0338
μ	1.3803	1.3030	1.2250	1.1280
$\overline{\mu}$	1.2280	1.1640	1.1070	1.0520
f_0	0.8900	0.9170	0.9430	0.9720
$\sqrt{f_\omega^2+f_A^2}$	0.8330	0.8520	0.8740	0.9130
$Y=\mu\cdot f_0\sqrt{f_\omega^2+f_A^2}$	1.025	1.018	1.010	1.0000
$Z=\frac{1}{Y}$	0.9756	0.9823	0.9900	1.0000

culated from $\overline{\mu}=\dfrac{1}{\sqrt{\left\{1-\left(\dfrac{\omega}{\nu_n}\right)^2\right\}^2+f_{An}{}^2}}$, assuming that added mass and damping force have constant value without concern to the frequency of the external force. Using $\nu_n=24.9$, $\bar{A}\fallingdotseq 0.5$ we obtain $f_{An}=0.197$ for this float. $\overline{\mu}$ is the magnification factor which is derived from by putting $e^{-k_0 T}=1$ and by neglecting the relative motion of the float and the wave in the equation (2).

Now if Xr_m denotes the relative displacement between the wave and the point $x=0$ of the float, relative variation ratio X is computed from the equation

$$X=\sqrt{Y^2+1-2Y\cos\varepsilon} \quad \cdots\cdots\cdots\cdots\cdots\cdots\cdots\cdots(20)$$

We obtain $Xr_m\fallingdotseq 1\,\text{mm}$ when $r_m=20\,\text{mm}$.

In this experiment as $\left|m'\dfrac{d^2y}{dt^2}+k_s y\right|$ was much smaller than $E_0\fallingdotseq 2\,\text{gr}$, the float operated sufficiently well.

[II] Additional calculation of $\bar{A}$ and K_4 for the Lewis form section

We computed $\bar{A}$ and K_4 at $H_0 = 2.0$ from [2] as the data for calculating the damping force and added mass at the light loading condition of the ship. Then it is published here additionaly (See Fig. 17, 18).

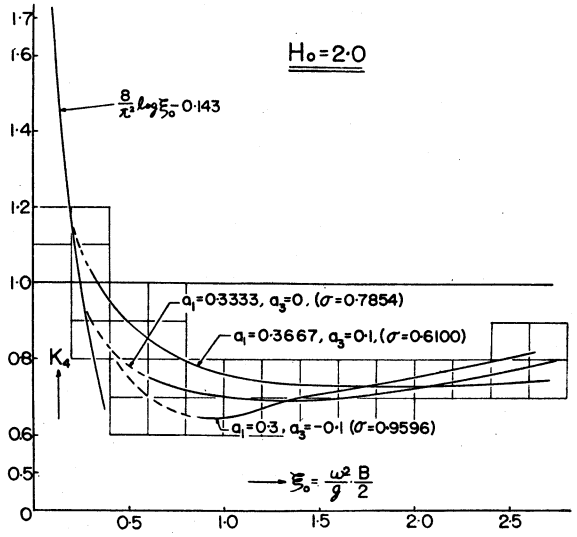

Fig. 17.

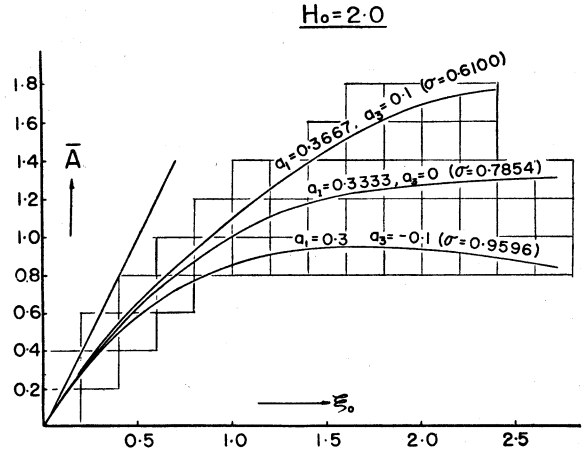

Fig. 18.

(Received March 26, 1960)

Reports of Research Institute for Applied Mechanics
Vol. VIII, No. 29, 1960

NOTE

The Time-Dependent Maxwellian Model of Solid Bodies

By Jun-ichi OKABE

1. It is well-known that the behavior of the Maxwellian model of solid bodies (see FIGURE 1) is defined by the equation

$$\dot{\varepsilon} = \frac{\dot{\sigma}}{E} + \frac{\sigma}{\eta}, \tag{1.1}$$

where ε = strain, $\dot{\varepsilon}$ = time rate of strain,
σ = stress, $\dot{\sigma}$ = time rate of stress,
E = modulus of elasticity, and η = coefficient of viscosity.

If we consider only the case of the constant time rate of strain, namely

$$\dot{\varepsilon} = \text{const.} \equiv \alpha, \tag{1.2}$$

in other words, denoting the time by t,

$$\varepsilon = \alpha t, \tag{1.3}$$

then (1.1) may be written

$$\dot{\sigma} + \frac{E}{\eta}\sigma = E\alpha, \tag{1.4}$$

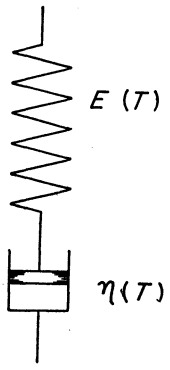

FIG. 1.

where both of E and η are the functions of the temperature of the solid body, T say, which arises in the course of the deformation owing to the internal friction of the body. The relationship between T and t will be formulated in a very complicated integro-differential equation, and we shall have to solve it together with (1.4). But to find the solution of these simultaneous equations in a general case being unfortunately impossible, the calculation which follows will be extremely simplified in order to avoid this difficulty.

Because the functional forms of $E(T)$ and $\eta(T)$ appearing in the equation (1.4) can be determined experimentally, we may regard E and η as dependent only upon t, at least conceptually, if the material, the mode of its deformation, and the condition surrounding the body have been specified definitely. Although both of these coefficients are known to decrease with T increasing, since that property is more conspicuous for η than for E, assuming for simplicity

$$E = \text{const.} \tag{1.5}$$

in our subsequent calculations, let us consider the *material* if the surrounding condition is to be prescribed, or on the contrary the *surrounding condition* if the material is specified, such that in the course of our constant strain rate deformation η of the material varies with t in the following manner:

$$\eta = \eta_1 + \frac{\eta_0 - \eta_1}{kt+1}, \qquad (1.6)$$
$$(\eta_0 > \eta_1 > 0, \quad k > 0.)$$

As readily found from (1.6),

$$\eta = \eta_0 \quad \text{at} \quad t = 0,$$
$$\eta = \eta_1 \quad \text{at} \quad t = \infty, \qquad (1.7)$$

and $$\frac{d\eta}{dt} = -k(\eta_0 - \eta_1) < 0 \quad \text{at} \quad t = 0.$$

In FIGURE 2 and TABLE 1 the behavior of the function $1/(kt+1)$ is shown for various values of k and t. Again (1.6) may be rewritten in the form

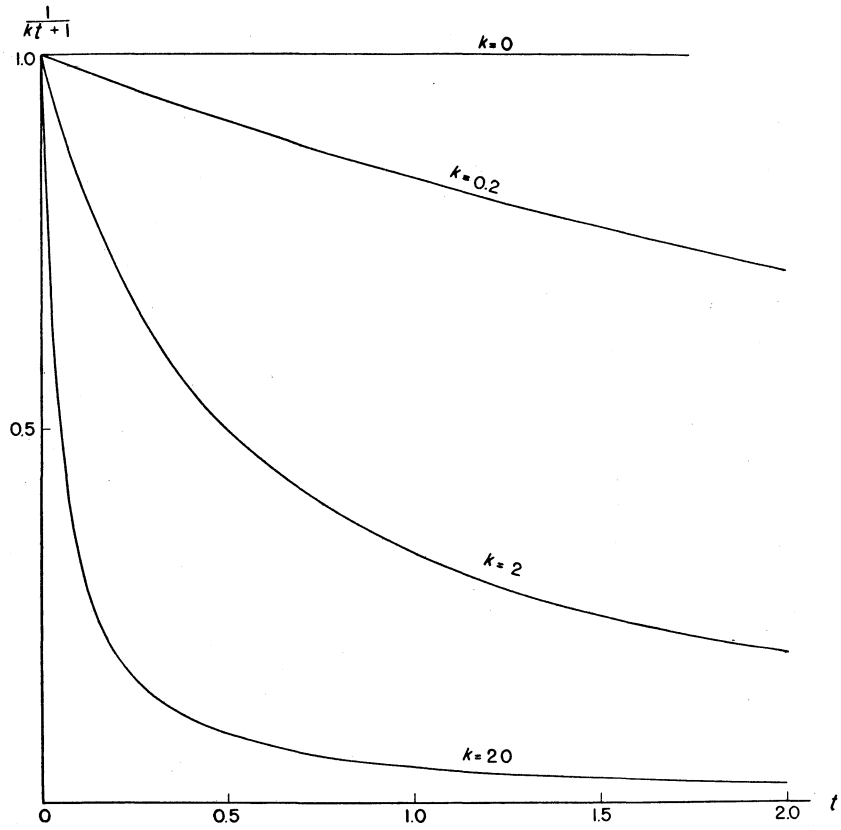

FIG. 2.

$$\eta = \eta_1 \frac{kt + \beta}{kt + 1}, \qquad (1.8)$$

where $$\beta \equiv \eta_0/\eta_1 > 1. \qquad (1.9)$$

Under the initial condition that

$$\sigma = 0 \quad \text{at} \quad t = 0, \qquad (1.10)$$

the solution of the equation (1.4) is obtained in the form

$$\sigma(t) = \exp\left(-\int_0^t \frac{E}{\eta} dt'\right) \int_0^t E\alpha \exp\left(\int_0^{t'} \frac{E}{\eta} dt''\right) dt', \quad (1.11)$$

and making use of the expressions (1.5) and (1.8), we are led to the result

$$\sigma(t) = e^{-\frac{E}{\eta_1}t} \left(\frac{kt+\beta}{\beta}\right)^{\frac{(\beta-1)E}{k\eta_1}} \int_0^t E\alpha e^{\frac{E}{\eta_1}t'} \left(\frac{kt'+\beta}{\beta}\right)^{-\frac{(\beta-1)E}{k\eta_1}} dt'. \quad (1.12)$$

Or putting

$$E/\eta_1 \equiv \gamma, \quad (1.13)$$

(1.12) is transformed into

$$\sigma(t) = E\alpha e^{-\gamma t} \left(\frac{k}{\beta}t+1\right)^{\frac{(\beta-1)\gamma}{k}} \int_0^t e^{\gamma t'} \left(\frac{k}{\beta}t'+1\right)^{-\frac{(\beta-1)\gamma}{k}} dt'. \quad (1.14)$$

However, the integral on the right-hand side being approximated by

$$\left(\frac{k}{\beta}t+1\right)^{-\frac{(\beta-1)\gamma}{k}} \int_0^t e^{\gamma t'} dt' \sim \left(\frac{k}{\beta}t+1\right)^{-\frac{(\beta-1)\gamma}{k}} \frac{e^{\gamma t}}{\gamma}$$

for a very large value of t, we have

$$\lim_{t\to\infty} \sigma = E\alpha/\gamma = \eta_1\alpha, \quad (1.15)$$

which is in accordance with the conclusion obtained directly from (1.4) when we put

$$\eta = \eta_1, \ \dot{\sigma} = 0 \quad \text{at} \quad t = \infty.$$

On the other hand, for the special case when

$$\eta = \text{const.} \equiv \eta_c, \text{ say,} \quad (1.17)$$

the solution of the equation (1.4) is readily found to be

$$\sigma(t) = \eta_c\alpha \ (1 - e^{-\frac{E}{\eta_c}t}), \quad (1.18)$$

and if we put

$$\eta_c = \eta_1 \quad (1.19)$$

specifically, we may write also

$$\sigma(t) = \eta_1\alpha \ (1-e^{-\gamma t}), \quad (1.20)$$

and

$$\lim_{t\to\infty} \sigma = \eta_1\alpha \quad (1.21)$$

as before.

Next, in order to transform (1.14) into more convenient form, let us introduce the new variable τ such that

$$\frac{k}{\beta}t + 1 \equiv \tau, \quad (1.22)$$

then it can be shown without difficulty that

$$\sigma(\tau) = E\frac{\alpha\beta}{k}\, e^{-\frac{\beta\gamma}{k}\tau}\, \tau^{\frac{(\beta-1)\gamma}{k}} \int_1^\tau e^{\frac{\beta\gamma}{k}\tau'}\, \tau'^{-\frac{(\beta-1)\gamma}{k}}\, d\tau', \tag{1.23}$$

from which we find

$$\begin{aligned}\sigma &> E\frac{\alpha\beta}{k} e^{-\frac{\beta\gamma}{k}\tau}\, \tau^{\frac{(\beta-1)\gamma}{k}}\, \tau^{-\frac{(\beta-1)\gamma}{k}} \int_1^\tau e^{\frac{\beta\gamma}{k}\tau'}\, d\tau' \\ &= E\frac{\alpha}{\gamma}\left\{1 - e^{-\frac{\beta\gamma}{k}(\tau-1)}\right\} \\ &= \eta_1\alpha\,(1 - e^{-\gamma t}).\end{aligned} \tag{1.24}$$

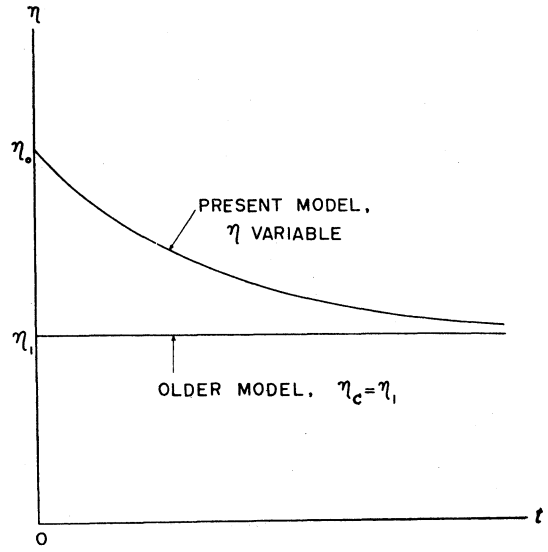

FIG. 3.

Namely, it has been proved that σ predicted from the present model is always larger than σ calculated by means of the older model.[1] (As the older model we mean the procedure in which both E and η are regarded as invariable. The behaviors of η's assumed in these two models are shown schematically in FIGURE 3.)

From (1.23) we can derive

$$\frac{d\sigma}{d\tau} = E\frac{\alpha\beta}{k}\left\{\frac{\sigma}{\eta_1\alpha}\left(\frac{\beta-1}{\beta\tau}-1\right)+1\right\}, \tag{1.25}$$

and

$$\frac{d^2\sigma}{d\tau^2} = E\frac{\alpha\beta}{k}\left\{\frac{d\sigma}{d\tau}\frac{1}{\eta_1\alpha}\left(\frac{\beta-1}{\beta\tau}-1\right) - \frac{\sigma}{\eta_1\alpha}\frac{\beta-1}{\beta\tau^2}\right\}. \tag{1.26}$$

If we denote the extreme value of σ (if any) by σ_m, the corresponding value of τ by τ_m, then from (1.25) σ_m satisfies the equation

[1] According to Professor Higuchi this result agrees with the experiment.

$$\frac{\sigma_m}{\eta_1\alpha} = \left(1 - \frac{\beta-1}{\beta\tau_m}\right)^{-1}, \tag{1.27}$$

so by virtue of the restriction

$$\infty > \tau_m \geqq 1, \tag{1.28}$$

it can be verified easily that

$$\beta \geqq \sigma_m/\eta_1\alpha > 1. \tag{1.29}$$

And further in the neighborhood of $\tau = \tau_m$, σ may be proved the ***maximum***, not the ***minimum***, since we have

$$\left(\frac{d^2\sigma}{d\tau^2}\right)_{\tau=\tau_m} = -E\frac{\alpha\beta}{k}\frac{\sigma_m}{\eta_1\alpha}\frac{\beta-1}{\beta\tau_m^2} < 0. \tag{1.30}$$

In conclusion, there are only two possibilities for the relationship between σ and τ, both of which are shown in FIGURE 4. Curves ① and ② represent respectively the results of the present, and the older, models.

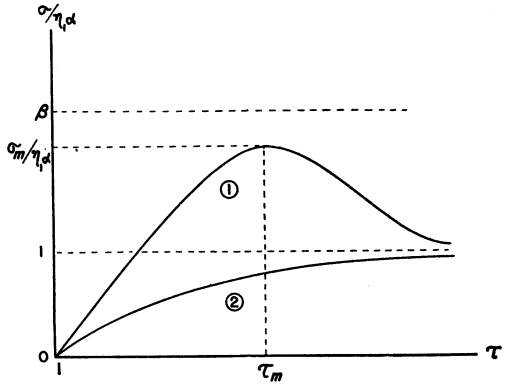

FIG. 4.

2. As the first example, let us consider the case

$$\begin{aligned} &\beta = 2, \quad \text{cf. (1.9)},\\ &\gamma = 2, \quad \text{cf. (1.13)},\\ &k = 2, \quad \text{cf. (1.6)}, \end{aligned} \tag{2.1}$$

where β, γ and k have the dimensions of (time^0), (time^{-1}), and (time^{-1}), respectively. Since

$$E = 2\eta_1 \tag{2.2}$$

numerically at present, it follows from (1.23) that

$$\sigma(\tau) = 2\eta_1\alpha e^{-2\tau}\tau\int_1^\tau e^{2\tau'}\frac{d\tau'}{\tau'}, \tag{2.3}$$

and by writing

$$2\tau \equiv \tilde{\tau}, \tag{2.4}$$

the above expression reduces to

$$\frac{\sigma(\tilde{\tau})}{\eta_1\alpha} = e^{-\tilde{\tau}}\,\tilde{\tau}\int_2^{\tilde{\tau}} e^{\tilde{\tau}'}\frac{d\tilde{\tau}'}{\tilde{\tau}'}, \tag{2.5}$$

where $\tilde{\tau}$ is connected with t by the equation

$$2t = \tilde{\tau} - 2. \tag{2.6}$$

Next, if the numerical values

$$\beta = 1.5, \quad \gamma = 2, \quad k = 2 \tag{2.7}$$

are assumed as the second example, we have as before from (1.23)

$$\frac{\sigma(\tilde{\tau})}{\eta_1\alpha} = e^{-\tilde{\tau}}\sqrt{\tilde{\tau}}\int_{1.5}^{\tilde{\tau}} e^{\tilde{\tau}'}\frac{d\tilde{\tau}'}{\sqrt{\tilde{\tau}'}} \tag{2.8}$$

where $1.5\,\tau = \tilde{\tau}$, (2.9)

so that $2t = \tilde{\tau} - 1.5$. (2.10)

On the other hand, when

$$\eta \equiv \eta_0 = \eta_1, \tag{2.11}$$

(1.20) reduces to

$$\frac{\sigma(t)}{\eta_1 \alpha} = 1 - e^{-2t}, \tag{2.12}$$

for these two cases above-mentioned, since γ has the same value in both of our examples.

In FIGURE 5 and TABLE 2, two kinds of $\sigma/\eta_1\alpha$ corresponding to the parameters (2.1) and (2.7) are shown for various values of t; the former case was worked out using the formulas (2.5), (2.6), and the latter was calculated with the aid of (2.8), (2.10). The result of (2.12) is referred to as "the older model" in the figure and the table for ready comparison. Since there exists a relationship given by (1.3) between the strain and the time, the abscissa of FIGURE 5 is proportional to the strain itself.

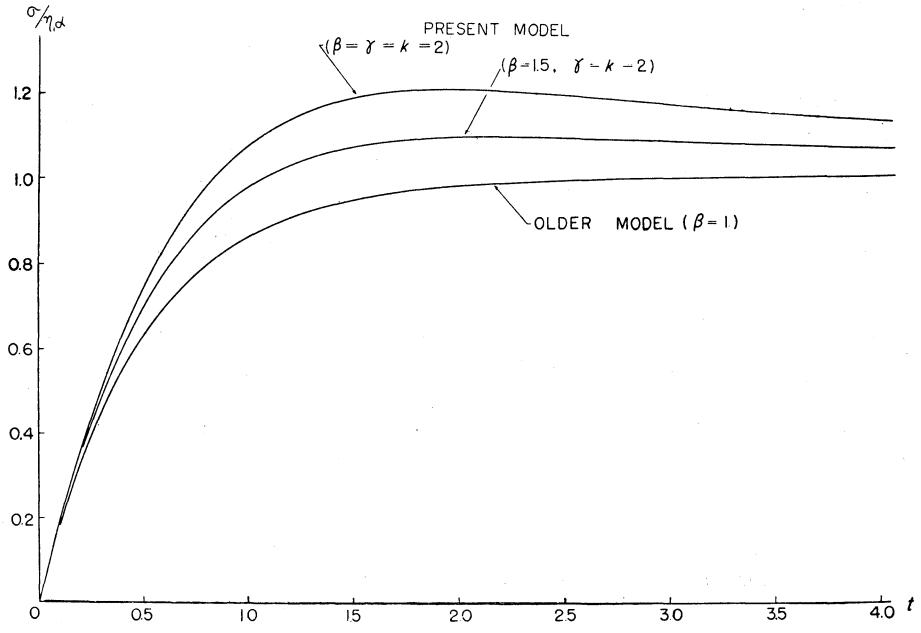

FIG. 5.

Finally, with a view to knowing the mode of variation of η with T, the temperature of the solid body, we denote by q the heat generated per unit time in the body per unit volume owing to the internal friction. Then, since q is proportional to the product of σ and $\dot{\varepsilon}$, the latter being constant and equal to α in our constant strain rate deformation, T at time t is found to be proportional to $\int_0^t \sigma\, dt$, provided that the specific heat of the body overall is independent of the temperature and that all the heat generated is stored in the body to elevate its temperature instead of escaping from it. Thus from (1.6), η and T are related to each other through t as the parameter. In FIGURE 6 and TABLE 3 for the values

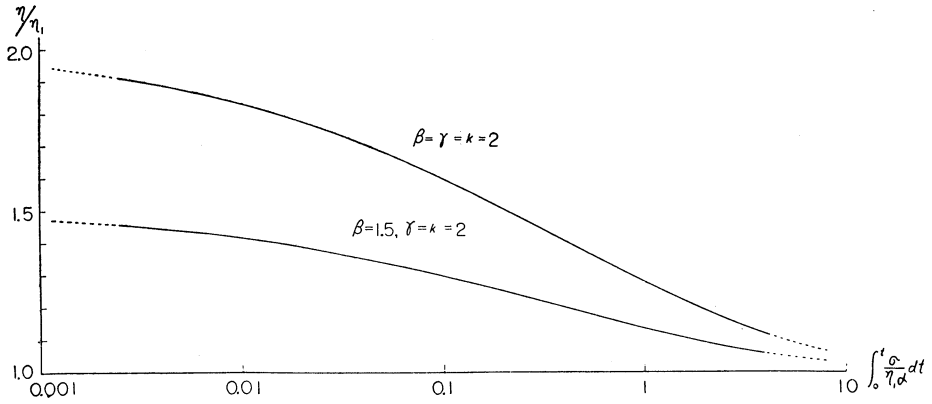

FIG. 6.

of the constants illustrated in the preceding two examples, the behavior of η/η_1 is shown as the function of $\int_0^t \sigma dt/\eta_1\alpha$ in the logarithmic scale.

The writer is very grateful to Professor M. Higuchi of the Institute for his advices and encouragements.

(Received January 16, 1960)

TABLE 1.

t	$1/(kt+1)$ $k=0.2$	$1/(kt+1)$ $k=2$	$1/(kt+1)$ $k=20$
0	1.0000	1.0000	1.0000
0.005	0.9990	0.9901	0.9091
0.01	0.9980	0.9804	0.8333
0.02	0.9960	0.9615	0.7143
0.03	0.9940	0.9434	0.6250
0.04	0.9921	0.9259	0.5556
0.05	0.9901	0.9091	0.5000
0.1	0.9804	0.8333	0.3333
0.2	0.9615	0.7143	0.2000
0.3	0.9434	0.6250	0.1429
0.4	0.9259	0.5556	0.1111
0.5	0.9091	0.5000	0.0909
0.6	0.8929	0.4545	0.0769
0.7	0.8772	0.4167	0.0667
0.8	0.8621	0.3846	0.0588
0.9	0.8475	0.3571	0.0526
1.0	0.8333	0.3333	0.0476
1.1	0.8197	0.3125	0.0435
1.2	0.8065	0.2941	0.0400
1.3	0.7937	0.2778	0.0370
1.4	0.7813	0.2632	0.0345
1.5	0.7692	0.2500	0.0323
1.6	0.7576	0.2381	0.0303
1.7	0.7463	0.2273	0.0286
1.8	0.7353	0.2174	0.0270
1.9	0.7246	0.2083	0.0256
2.0	0.7143	0.2000	0.0244

TABLE 2.

t	$\sigma/\eta_1\alpha$ (present model) $(\beta=\gamma=k=2)$	$\sigma/\eta_1\alpha$ (present model) $(\beta=1.5, \gamma=k=2)$	$\sigma/\eta_1\alpha$ (older model)
0	0	0	0
0.025	0.0494	0.0492	0.0488
0.050	0.0975	0.0967	0.0952
0.075	0.1443	0.1425	0.1393
0.100	0.1897	0.1867	0.1813
0.125	0.2339	0.2294	0.2212
0.150	0.2767	0.2704	0.2592
0.175	0.3183	0.3098	0.2953
0.200	0.3585	0.3478	0.3297
0.225	0.3974	0.3842	0.3624
0.250	0.4350	0.4192	0.3935
0.275	0.4713	0.4528	0.4231
0.300	0.5063	0.4850	0.4512
0.325	0.5401	0.5159	0.4780
0.350	0.5727	0.5454	0.5034
0.375	0.6041	0.5737	0.5276
0.400	0.6343	0.6008	0.5507
0.425	0.6633	0.6267	0.5726
0.450	0.6912	0.6515	0.5934
0.475	0.7180	0.6752	0.6133
0.500	0.7438	0.6978	0.6321
0.525	0.7684	0.7193	0.6501
0.550	0.7921	0.7399	0.6671
0.575	0.8148	0.7596	0.6834
0.600	0.8365	0.7783	0.6988
0.625	0.8573	0.7962	0.7135
0.650	0.8772	0.8132	0.7275
0.675	0.8962	0.8294	0.7408
0.700	0.9143	0.8448	0.7534
0.725	0.9316	0.8595	0.7654
0.750	0.9482	0.8734	0.7769
0.775	0.9639	0.8867	0.7878
0.800	0.9789	0.8993	0.7981
0.825	0.9932	0.9113	0.8080
0.850	1.0068	0.9227	0.8173
0.875	1.0198	0.9335	0.8262
0.900	1.0321	0.9437	0.8347
0.925	1.0437	0.9534	0.8428
0.950	1.0548	0.9626	0.8504
0.975	1.0653	0.9713	0.8577
1.000	1.0752	0.9795	0.8647
1.050	1.0936	0.9947	0.8775
1.100	1.1099	1.0083	0.8892
1.150	1.1245	1.0204	0.8997
1.200	1.1374	1.0311	0.9093
1.250	1.1488	1.0406	0.9179
1.300	1.1587	1.0490	0.9257
1.350	1.1674	1.0564	0.9328
1.400	1.1750	1.0629	0.9392
1.450	1.1814	1.0686	0.9450

TABLE 2. *continued*

t	$\sigma/\eta_1\alpha$ (present model) $(\beta = \gamma = k = 2)$	$\sigma/\eta_1\alpha$ (present model) $(\beta = 1.5, \gamma = k = 2)$	$\sigma/\eta_1\alpha$ (older model)
1.500	1.1869	1.0735	0.9502
1.550	1.1915	1 0778	0.9550
1.600	1.1954	1.0814	0.9592
1 650	1.1985	1.0845	0.9631
1.700	1.2009	1.0871	0.9666
1.750	1.2028	1.0893	0.9698
1.800	1.2041	1.0911	0.9727
1.850	1.2050	1.0925	0.9753
1.900	1.2054	1.0936	0.9776
1.950	1.2055	1.0944	0.9798
2.000	1.2052	1.0950	0.9817
2.100	1.2038	1.0955	0.9850
2.200	1.2014	1.0953	0.9877
2.300	1.1984	1.0945	0.9899
2.400	1.1948	1.0934	0.9918
2.500	1.1908	1.0919	0.9933
2.600	1.1865	1.0902	0.9945
2.700	1.1821	1.0884	0.9955
2.800	1.1776	1.0864	0.9963
2.900	1.1731	1.0844	0.9970
3.000	1.1686	1.0824	0.9975
3.100	1.1641	1.0803	0.9980
3.200	1.1597	1.0783	0.9983
3.300	1.1554	1.0763	0.9986
3.400	1.1513	1.0744	0.9989
3.500	1.1473	1.0725	0.9991
3.600	1.1434	1.0706	0.9993
3.700	1.1396	1.0688	0.9994
3.800	1.1360	1.0671	0.9995
3.900	1.1325	1.0654	0.9996
4.000	1.1292	1.0638	0.9997

TABLE 3.

t	$\beta = \gamma = k = 2$		$\beta = 1.5,\ \gamma = k = 2$	
	$\int_0^t \sigma\, dt/\eta_1\alpha$	η/η_1	$\int_0^t \sigma\, dt/\eta_1\alpha$	η/η_1
0	0	2.000	0	1.500
0.05	0.00246	1.909	0.00244	1.455
0.10	0.00966	1.833	0.00956	1.417
0.15	0.0213	1.769	0.0210	1.385
0.20	0.0372	1.714	0.0365	1.357
0.25	0.0571	1.667	0.0557	1.333
0.30	0.0807	1.625	0.0783	1.313
0.35	0.1077	1.588	0.1041	1.294
0.40	0.1378	1.556	0.1328	1.278
0.45	0.1710	1.526	0.1641	1.263
0.50	0.207	1.500	0.1979	1.250
0.55	0.245	1.476	0.234	1.238
0.60	0.286	1.455	0.272	1.227
0.65	0.329	1.435	0.312	1.217
0.70	0.374	1.417	0.353	1.208
0.75	0.420	1.400	0.396	1.200
0.80	0.468	1.385	0.440	1.192
0.85	0.518	1.370	0.486	1.185
0.90	0.569	1.357	0 533	1.179
0.95	0.621	1.345	0.580	1.172
1.0	0.675	1.333	0.629	1.167
1.1	0.784	1.313	0.728	1.156
1.2	0.896	1.294	0.830	1.147
1.3	1.011	1.278	0.934	1.139
1.4	1.128	1.263	1.040	1.132
1.5	1.246	1.250	1.147	1.125
1.6	1.365	1.238	1.255	1.119
1.7	1.485	1.227	1.363	1.114
1.8	1.605	1.217	1.472	1.109
1.9	1.726	1.208	1.581	1.104
2.0	1.846	1.200	1.691	1.100
2.2	2.09	1.185	1.910	1.093
2.4	2.33	1.172	2.13	1.086
2.6	2.56	1.161	2.35	1.081
2.8	2.80	1.152	2.56	1.076
3.0	3.04	1.143	2.78	1.071
3.2	3.27	1.135	3.00	1.068
3.4	3.50	1.128	3.21	1.064
3.6	3.73	1.122	3.43	1.061
3.8	3.96	1.116	3.64	1.058
4.0	4.18	1.111	3.85	1.056

ERRATA

Reports of Research Institute for Applied Mechanics

Vol, VII, No. 26, 1959

Page 76, line 2, from the bottom, for "(1 8)" read "(1.8)."
Page 85, line 7, from the bottom, for "J_1'' ($j_{0\,n}$)" read "$J_1''(j_{0,n})$."
Page 87, line 12, for "approximata" read "approximate."
Page 99, TABLE 1, $x = 1.0$, $t = 1.5$, for "0 777" read "0.777."
Page 100, TABLE 3, ($\tau = 0$; $\mu = 50$), $n = 22$, for "$-$0. 80 5543" read "$-$0.0080 5543."
Page 102, TABLE 5, ($\tau = 1$; $\mu = 30$), $n = 6$, for "$-$0 0336 7637" read "$-$0.0336 7637."
Page 110, $\sigma = 0.725$, for "0 372 803" read "0.372 803," $\sigma = 0.800$, for "0 267 960" read "0.267 960," and σ=0.975, for "0 076 278" read "0.076 278."
Page 111, footnote, for "$j_{0\,8} = 24{,}35\cdots$" read "$j_{0,8} = 24.35\cdots$."
Page 113, footnote, for "$j_{0\,16}$" and "$j_{0\,17}$" read "$j_{0,16}$" and "$j_{0,17}$" respectively.
Page 114, footnote, for "$j_{0\,21}$" and "$j_{0\,23}$" read "$j_{0,21}$" and "$j_{0,23}$" respectively.
Page 115, $\sigma = 0.225$, for "0 024 413" read "0.024 413," σ=0.575, for "$-$0,105 24" read "$-$0.105 24," and footnote, for "$j_{0\,26}$" read "$j_{0,26}$."
Page 117, footnote, for "$j_{0\,36}$" and "$j_{0\,39}$" read "$j_{0,36}$" and "$j_{0,39}$" respectively.
Page 121, equation (39), for "ζ_2" read "ζ^2."
Page 129, TABLE 17, $\vartheta = -0.5$, $\sigma = 0.5$ ($R = 1$) for "0 0416" read "0.0416." (*J. O.*)